

Maximilian Schmid, BSc

Elucidation of the correlation between process and substrate conditions, morphology and enzyme production in *T. reesei*

MASTER'S THESIS

to achieve the university degree of
Diplom-Ingenieur
Master's degree programme: Biotechnology

submitted to
Graz University of Technology

Supervisor
Univ.-Prof. Dipl.-Ing. Dr.techn. Bernd Nidetzky
Institute of Biotechnology and Biochemical Engineering

Graz, September 2015

AFFIDAVIT

I declare that I have authored this thesis independently, that I have not used other than the declared sources/resources, and that I have explicitly indicated all material which has been quoted either literally or by content from the sources used.

The text document uploaded to TUGRAZonline is identical to the present master's thesis.

Date

Signature

Kurzfassung

Die Produktion von (Hemi-) Cellulasen, welche für eine effiziente Depolymerisierung von Zellulose und Hemizellulose benötigt werden, ist eine der Hauptschwierigkeiten bei der Produktion von Biotreibstoffen und Plattformchemikalien. Der für die Enzymproduktion am meisten verwendete Organismus ist *Trichoderma reesei* (*T. reesei*). In Abhängigkeit der Wachstumsbedingungen können filamentöse Pilze verschiedene Micro- (z.B. Form der Hyphen, Verzweigungsgrad) und Makromorphologien (Pellets und filamentöses Wachstum) ausbilden. Vorangegangene Studien mit *Aspergillus spp* haben gezeigt, dass die Morphologie des Organismus die Produktivität direkt beeinflussen kann. Das Ziel dieser Studie ist es, den multidimensionalen Zusammenhang von Substrat, Prozessbedingungen, Mikromorphologie und Enzymproduktion von zwei *T. reesei*-Mutanten zu untersuchen. Die Studie umfasste sowohl Schüttelkolben- und Bioreaktorfermentationen als auch Methoden zur Bestimmung der Enzymaktivität und die Micromorphologieanalyse mit Hilfe des Confocal Laser Scanning Mikroskops (CLSM). Die CLSM Bilder wurden mit einem eigens für diese Studie entwickeltem MATLAB-Programm ausgewertet. So konnte in dieser Studie ein klarer Zusammenhang zwischen Micromorphologie und Enzymproduktion festgestellt werden.

Abstract

The production of (hemi-) cellulolytic enzymes, required for efficient de-polymerization of cellulose and hemicellulose, is one of the major bottlenecks in the production of biofuels and platform chemicals from lignocellulosic materials. *Trichoderma reesei* is the most commonly applied organism for the production of (hemi-) cellulases. As all filamentous fungi, *T. reesei* forms different micro (e.g. hyphae length and width, degree of branching) and macro (pelletized and dispersed growth) morphologies, dependent on the provided cultivation conditions. It is known from other filamentous fungi, e.g. *Aspergillus* spp., that the morphology is directly influencing yields and productivities of the desired product. Aim of this study was therefore, to investigate the multidimensional relationship between substrate and process conditions, micromorphology and enzyme yield in two *T. reesei* mutant strains. The laboratory work thereby provided an insight into fermentation technologies as well as analytical methods such as the determination of enzymatic activities. Further, a novel method for analysis of the fungal micromorphology was developed, utilizing Confocal Laser Scanning Microscopy (CLSM) as imaging technique and a specially designed MATLAB program. By applying CLSM and newly designed program a correlation between the micromorphology and enzyme activities could be detected.

Index

1	Introduction.....	1
1.1	Enzyme production.....	2
1.1.1	<i>Trichoderma reesei</i>	2
1.1.2	Cellulose degradation machinery of <i>T. reesei</i>	3
1.2	Morphology.....	3
1.2.1	Filamentous fungi.....	3
1.3	Correlation between morphology – cellulose production and Process conditions.....	5
2	Materials & Methods.....	7
2.1	Materials.....	7
2.1.1	Cultivation media.....	7
2.1.2	Confocal Laser Scanning Microscope.....	7
2.1.3	Enzyme activity.....	8
2.2	Instruments.....	9
2.3	Methodes.....	10
2.3.1	Agar plate.....	10
2.3.2	Spore harvest.....	10
2.3.3	Fermentation.....	10
2.3.4	Morphology analysis.....	10
2.3.5	Enzyme activity.....	11
3	Results and Discussion.....	13
3.1	Optimization of analysis.....	14
3.2	Differences in morphology in dependence of fermentation conditions and strain.....	15
3.3	Fungal morphology influences the level of enzyme secretion by <i>T. reesei</i> strains.....	24
4	Conclusion.....	31
5	Literature.....	33
	List of figures.....	35
	Table.....	36
6	Index of abbreviations.....	37
7	Appendix.....	38
7.1	rotein, Beta-Glucosidase activity and Xylanase activity at 150 rpm.....	38
7.2	Evaluation of the CLSM picture.....	39

1 Introduction

Rising energy consumption has shifted the focus of energy generation towards renewable sources. One of the most important applications is the production of ethanol from biomass, which can contribute to a sustainable development. These resources are locally available and conversion to useable energy is possible without high capital investments. Any material that contains sugar could be used to produce ethanol. The raw materials can be divided into three main types: sugar, starch and cellulose materials [1]. In 2008 approximately 90% of the global ethanol fuel production was concentrated in two countries, Brazil and the United States of America. In Brazil most of ethanol is produced from cane juice, whereas in the USA ethanol is usually produced from corn.

The need of a non-food dependent source led to the development of the 2nd generation of biofuels, using lignocellulosic materials as feedstock.

Various sources exist such as wood residues, spent vegetable oil or algae. Wood residues are by far the largest source of biomass currently available. The residues are gained from paper mills, sawmills and agriculture wastes. In the past, these materials were treated as waste in many countries. There are also some dedicated energy crops, mostly short-rotation woody crops, like tall grasses. These grasses are most promising because of their ability to obtain numerous harvests from one single planting, which helps to significantly decrease the cost and the area needed for production [1].

Lignocellulose is the major structural component of all plant cell walls. It consists of three major components: cellulose (40-50%), hemicellulose (25-35%) and lignin (15-20%) and is extremely recalcitrant [2]. Cellulose, the most abundant organic molecule on Earth, is a linear biopolymer of anhydroglucopyranose-molecules which are connected via a β -1,4-glycosidic bonds. Adjacent cellulose chains are connected by hydrogen bonds, Van der Waal's forces and hydrophobic interactions. This leads to a parallel alignment of crystalline structures known as microfibrils. Hemicellulose consists of heterogeneous polymers of pentoses (e.g. xylose and arabinose), hexoses (mainly mannose, glucose and galactose) and sugar acids. The composition of hemicellulose varies between different plant species. The third main polymer of lignocellulose is lignin. It generally contains three aromatic alcohols including coniferyl alcohol, sinapyl and p-coumaryl. The main purpose of lignin is to act as a barrier for any solution or enzymes by linking to both hemicellulose and cellulose. This prevents penetration of lignocellulytic enzymes to the interior structure. As a result, lignin is the most recalcitrant component of lignocellulosic material [3].

To disrupt the complex structure of lignocellulose and to remove the lignin, a pre-treatment is necessary in the 2nd generation bioethanol production process. The goal is to reduce the level of crystalline cellulose in the structure and to increase the specific surface. The increase of the surface is

essential to maximize the yield of monomeric sugars gained from the hydrolysis. For the pre-treatment physical or chemical methods are available.

The pre-treated material is then hydrolysed by cellulase enzymes, converting the sugar polymers to free sugar molecules. The enzymes can be produced by fungi and bacteria. The gained sugars are converted into alcohol via baker's yeast. The ethanol can be blended with gasoline to obtain an oxygenated fuel with lower hydrocarbon and green house emission [4].

Production of the (hemi-) cellulolytic enzymes constitutes the economic bottleneck of 2nd generation biofuel production. Thus, it is important to increase the yield and productivity of enzyme production by simultaneously lowering the costs. Strategies so far targeted at genetic modification of the production organisms, as well as at the optimization of the growth conditions [5]. As it will be discussed in more detail hereinafter, enzyme secretion takes place during tip growth by majority [6]. Bhargava et al have shown with *Aspergillus oryzae*, that it is possible to improve protein production by controlling the fungus morphology [7].

Filamentous organism like *Trichoderma reesei* (*T. reesei*) are widely used for the production of proteins on industrial scale, due to their ability to produce and secrete large amounts of proteins. One of the most important applications is, to produce (hemi-) cellulolytic enzymes required for the transformation of agriculture wastes into fermentable sugars. As the saccharification of cellulolytic substrate is a major cost factor, it is most important to understand the relationship between morphology, process conditions and protein production in order to increase the protein production.

1.1 Enzyme production

1.1.1 *Trichoderma reesei*

In nature only a small number of organisms have been discovered to utilize lignocellulose as energy source. One of the most interesting sources of cellulolytic enzymes is *T. reesei*. The first attempt of generating a high cellulase-producing mutant strain, QM6a, was described by Mandels et al., 1971 [8]. Strain QM9124 produced twice as much cellulases as the original wild-type. Further UV irradiation resulted in the most commonly used strain QM9414 [9]. On the other hand QM9414 is still catabolite-repressed. To overcome the catabolite repression new mutants were created like Δ Cre. Previous studies have described it as useful enzyme producer at both laboratory and pilot scale. Little is still known how Cre1 is acting in the presence of more complex carbon sources, like cellulose. The *T. reesei* mutant used in this study is called Δ Cre and was produced by Portnoy et al. This mutant shows a reduced growth rate, smaller colonies and less spores [10].

1.1.2 Cellulose degradation machinery of *T. reesei*

The complex structure of lignocellulose structure inhibits an efficient conversion to simple sugars. To overcome this problem, various different types of enzymes are required for degradation. Those enzymes are summarized as cellulase enzymes. The cellulolytic system of *T. reesei* consists of three

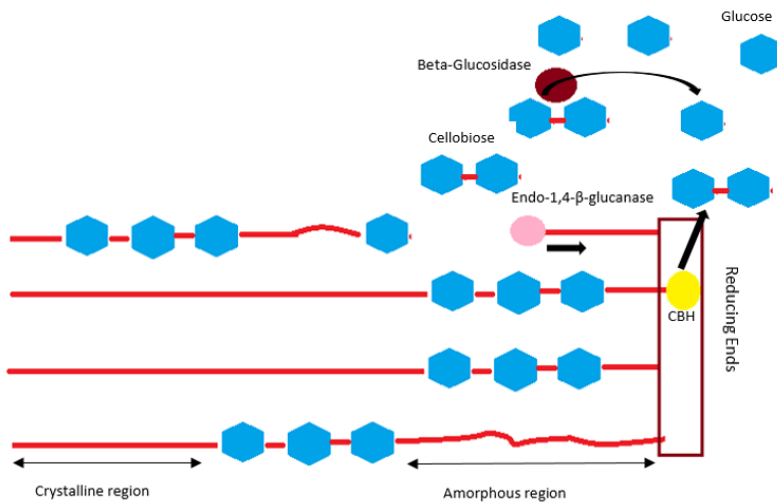


Figure 1: Cellulose degrading system of *T. reesei*

major enzyme classes, exoglucanases, endo-1,4-β-glucanases and β-glucosidases. Exoglucanases, in the case of *T. reesei* they are called cellobiohydrolases (CBH), liberate D-glucose dimers (cellobiose) from the end of the cellulose chain. Endoglucanases (EG) are cutting randomly within the cellulose. The secretion and the degradation processes take place simultaneously. The limiting step of the

degradation is the depolymerisation of the insoluble crystalline cellulose by CBHs and EGs [5].

1.2 Morphology

1.2.1 Filamentous fungi

Filamentous fungi are morphologically complex organisms rendering fungal fermentations difficult in terms of broth rheology, enzyme production and fungal morphology. It is necessary to understand the interrelation between these parameters in order to improve the enzyme production. The fungal biomass is formed from spores and goes through various differentiating steps. The morphology can be classified into dispersed and pelleted forms. According to V. Lecaet et al., under the operating conditions leading to cellulase production, *T. reesei* is mainly found in the disperse form [11]. These fermentations include freely dispersed mycelia and clumped mycelia [11]. The morphology can have a significant effect on the fermentation broth rheology and thus the performance of the bioreactor. Ongoing filamentous growth results in highly viscous broths with non-Newtonian, pseudoplastic flow behaviour. The high viscosity has a negative impact on the mass transfer properties, especially the gas-liquid mass transfer. The morphology, in turn, is influenced via gas flow rate, rotation speed and temperature [12].

Micromorphology

When enough nutrients are available, microbial organisms have the ability to grow exponentially, which requires that all or a constant percentage of cells contribute to biomass growth. If it is assumed that all growth takes place in the hyphae and that individual hyphae extend at a constant rate, exponential growth is only possible if new branches are produced.

According to Prosser et al., the first branch is formed from the germ tube towards the end of the exponential extension [13]. The branch is supported by material provided by a parent hyphae. These materials, precursors for the cell as well as proteins involved in cell-wall synthesis, are transported in vesicles from the endoplasmic reticulum (ER) to the tip of the hyphae. This transport, working at constant velocity, is likely to be the limiting step of elongation. The vesicles are accumulated at the apex and form the so called Spitzenkörper (SP). The SP determines the shape of the tubular shape as well as the growth direction of the cell [14].

The length of the hyphae increases until it reaches a constant value which, in young mycelia, is equal to that of the parent hypha. The newly formed tips can also branch, resulting in the formation of new extending tips [6]. It has been shown with *Aspergillus nidulans* that the first septa divides the cell into an apical and subapical part. The apical compartment is located at the tip and is able to exchange cytoplasm with the subapical part [14]. During growth of the apical cell, the length of the subapical cell

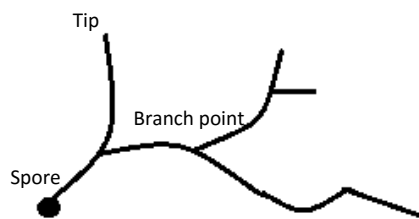


Figure 2: Growing mycelium with several tips

is constant. With ongoing elongation more septa are formed and the apical compartment becomes a subapical part, while the previous subapical cells turn into hyphae. Over the time vesicles accumulate in the subapical cell, which cannot pass a septa, leading to the formation of a branch. These differentiation of the hyphae in parts with various metabolic activities leads to the production of secondary metabolites in the growth-arrested parts, while the growth associated proteins are synthesized in the active part of the cell [14].

However, according to Bocking et al [15], no correlation is found between the number of tips and protein secretion.

Macromorphology

The macromorphology directly results from micromorphology events. In submerged cultivation two

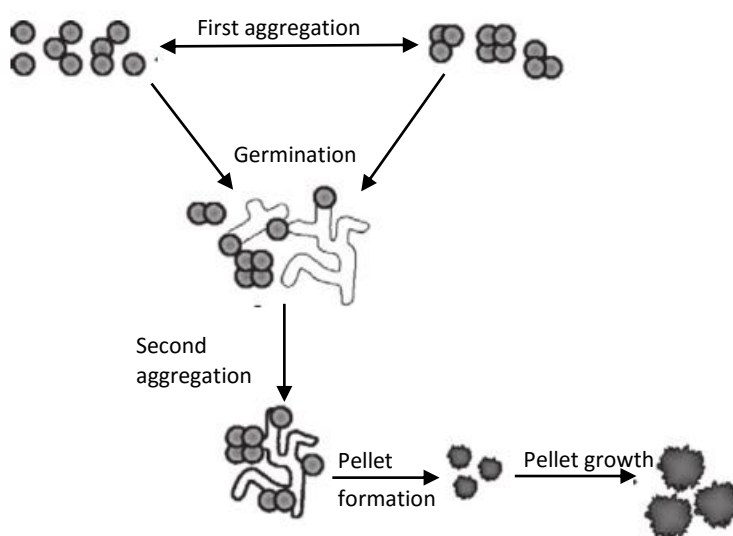


Figure 3 Aggregation model for coagulation filamentous microorganisms [14]

different forms are observed, the dispersed and the pelleted form. The pellets are formed when mycelia grow into a stable, more or less branched spherical aggregates consisting of intertwined network of hyphae. [14].

After the inoculation, spores aggregate until a steady-state condition, between aggregation and disintegration of conidial packages, is reached. Next the germination and hyphal growth disrupts the

aggregation and increases the surface area of the hyphae. The second aggregation step is triggered as conidia attach to hyphae. During the second aggregation step further spores attach to the conidia, resulting finally in the formation of pellets. A key parameter for the pellet formation is mass transport across the aggregates, which can be divided into three key processes: mass transfer from the bulk phase to the surface of the pellet, transport to the core of the aggregate and the turnover rates within the pellet. Each of these processes has the possibility to be a limiting step during biomass growth. The pellet density is changing over time during cultivation as the nutrient transport differs with the size of the pellet [14].

1.3 Correlation between morphology – cellulose production and process conditions

As mentioned above the morphology of filamentous fungi varies between the pelleted and the dispersed form. Submerge cultures consists of branched and unbranched hyphae and aggregates. The assumption is that the morphology of the fungi and cellulase production interact. Therefore the cellulase may depend on optimal process conditions as well as optimal morphology. Therefore the assumption was created, that process-conditions, morphology interact with each other.

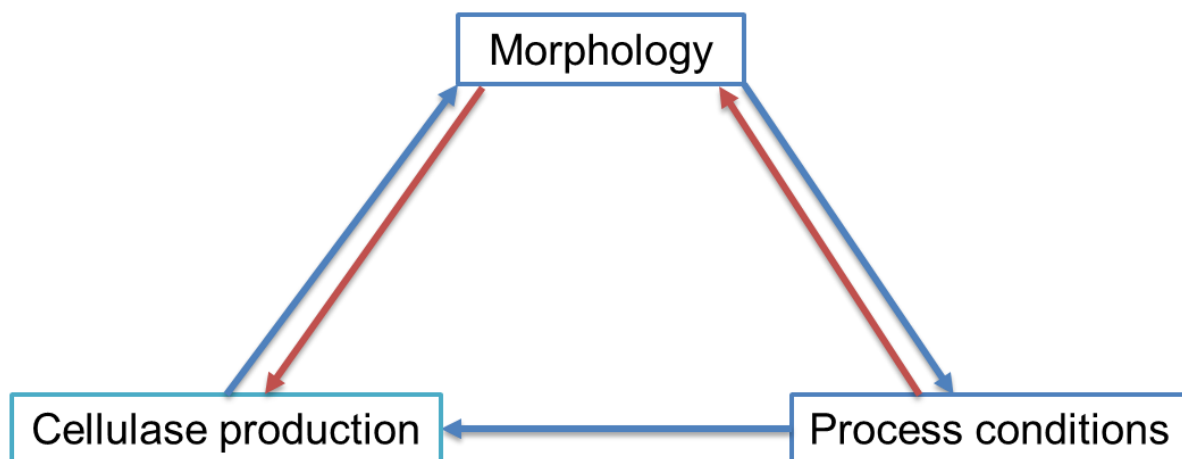


Figure 4: Relationship between process conditions, morphology and cellulase production.

To increase the productivity, the relationship between operational conditions and fungal morphology must be known [16]. The investigation of the relationship between fungal morphology and product formation is difficult, as the system consists of many interrelated factors. Bhargava et al have shown with *Aspergillus oryzae* that it is possible to improve protein production by controlling the fungus morphology [7]. It is commonly accepted that protein secretion of filamentous fungi occurs at the tip of growing hyphae [6], since the tips of the growing fungi are most active. This lead to the assumption, that an increase in active tip number would improve protein production. In conclusion the enzyme secretion is higher at the hyphae tips, where the cell wall is more porous than in the mature wall which allows a rapid diffusion of proteins. Increasing the number of active tips should therefore increase the enzyme production. This may be influenced with the optimization of process-conditions. However,

according to Booking et al., no evidence was found that there is a correlation between the number of tips and protein secretion [15]. While Wongwicharn et al. described an increased secretion of heterologous hen egg white lysozyme by a more branched mycelium of *Aspergillus niger* [17].

Different approaches to change fungal morphology in *T. reesei* cultivations have been described in literature.

The morphology can, for an instance, be changed by varying inoculation methods. The inoculation is usually accomplished, using agar pieces over grown with fully developed fungi. The inoculation method was developed by Doppelbauer et al [18]. This method implies that the hyphae are already branched and the mycelium has started to grow. Another method of inoculation is to directly add spores to the fermentation media. Thus, F.C. Domingues et al, have shown that different media and spore concentration have an influence on morphology. The result was that a high spore concentration leads to filamentous mycelium and a low concentration produce pellets [16]. However, this study did not reveal if the reported change in morphology has an influence on the cellulose production and information on the relationship between fungal morphology and cellulose expression in *T. reesei* are scarce in literature in general.

In this study, the change of morphology in dependence of inoculation method, substrate and process conditions is analyzed. To quantify morphology changes, the length and width of septa as well as the level of branching was determined. Further, the influence of morphological changes on enzyme activity, e.g. total cellulose activity and xylanase activity, was elucidated.

2 Materials & Methods

2.1 Materials

2.1.1 Cultivation media

Potato dextrose agar (Carl Roth GmbH + Co. KG) was prepared as recommended by the manufacturer

Table 1: Mineral Media (M-Media)

Reagents	Concentration
KH ₂ PO ₄	5 g/pL
Yeast extract	5 g/L
(NH ₄) ₂ SO ₄	0.75 g/L
MgSO ₄ x H ₂ O	0.3 g/L
Wheat straw	14 g/L
CaCl ₂ x 2H ₂ O	0.3 g/L
Trace elements	1 mL/L

Table 2: Trace elements

Mix	Concentration	pH-Value
FeSO ₄ x 7 H ₂ O	5 g/L	
MnSO ₄ x H ₂ O	1.6 g/L	
ZnSO ₄ x 7 H ₂ O	1.4 g/L	
CoCl ₂ x 6 H ₂ O	2 g/L	
EDTA-Na ₂	15 g/L	Before adding EDTA pH was set to 8. After adding EDTA pH was set to 4.

2.1.2 Confocal Laser Scanning Microscope

Table 3: Carbonate-bicarbonate buffer pH 9.2 (C-buffer)

Reagents	Concentration
Sodium carbonate (Na ₂ CO ₃)	50 mM
Sodium bicarbonate (NaHCO ₃)	50 mM

Table 4: Calcoflour white stain

Reagents	Concentration	Media
Calcoflour white	0.001 %	H ₂ O

Table 5: Acridin Orange

Reagents	Concentration	Media
Fluorescence brightener	0.001 %	H ₂ O
Acridine orange	6 µg/mL	<ul style="list-style-type: none"> • Citric acid 0.1 M • Na₂HPO₄ 0.2 M pH 2.6

2.1.3 Enzyme activity

Table 6: β-glucosidase Assay

Reagents	Concentration	pH-Value
Sodium-carbonate	1 M	
Sodium-acetate-buffer (Na-Ac)	50 mM	5
p-Nitrophenol (p-NP)	1 mM in Na-Ac buffer	
p-Nitrophenol-glucopyranosid (P-nPG)	2 mM in Na-Ac buffer	

Table 7: Bradford assay

Reagents	Concentration	pH-Value
Potassium phosphate (KPh)	500 mM	7.4
Calcium chloride (CaCl ₂)	250 mM	
EtOH	Pure ethanol (analytical grade)	
H ₂ O	Filtered millipore water	

Table 8: Xylanase assay

Reagents	Concentration	pH-Value
Sodium-citrate buffer	50 mM	4.8-5.3
Birchwood xylan	1 g	
Dinitrosalicylic acid solution		

Filter Paper Activity (FPA)

Table 9: Dinitrosalicylic acid solution (DNS)

Reagents	Concentration
Distilled water	708 mL
3,5-Dinitrosalicylic acid	5.3 g
NaOH	9.9 g
Rochelle salts	153 g
Phenol	3.8 g
Na ₂ SO ₃	4.2

Table 10: Citrate buffer

Reagents	Concentration	pH-Value
Sodium-citrate	50 mM	4.8

Filterpaper: 1x4cm piece of cellulose filter paper Whatman No 1

2.2 Instruments

- Photometer
 - Plate reader: FLUOstar Omega
 - Beckmann Coulter DU800 Spectrophotometer
- Incubator: Satorius stedim Certomat BS1
- Centrifuge
 - Eppendorf 5810R
 - Eppendorf 5424R
- Thermomixer: Eppendorf Thermomixer comfort
- Workbench: Bioair AURA 200 M.A.C.4
- Weight stations:
 - Satorius LE244S
 - Satorius BP160P
 - Akkulab satoriusgroup Vicon
- pH meter: WTW series inoLAB pH 720
- Autoclave:
 - Varioklav
 - Federgari
 - Systec 5075ELV
- Waterbath: Bartelt GFL1083
- Bioreactor: Infors HT Labfors
- Microscope: Leica TCS SPE; Confocal Laser Scanning Microscope Leica DM5500 Q

2.3 Methodes

2.3.1 Agar plate

The *T. reesei* Δ Cre strain and QM9414 strain were revitalized on PDA plates and incubated at 30 °C for 4 days.

2.3.2 Spore harvest

T. reesei strains were grown on potato dextrose agar (PDA) plates. The plates were incubated at 30°C for 10 days for QM9414 and 24 days for the Δ Cre mutant until fungi sporulated. The spores were harvested by washing the PDA plates with 10 mL of sterile water containing 1% Triton X-100. The spore solution was stored at 4°C. The spore concentration was determined by using Thoma chambers [6].

2.3.3 Fermentation

For the preculture of QM9414 and Δ Cre M-Media was prepared with glucose as C-source. After 2 days the fungal biomass was harvested by centrifugation. 40 mg of biomass were prepared for inoculation of the main cultures.

Shaken flask cultivations

For the fermentation of the *T. reesei* strains QM9414 and Δ Cre M-media was prepared. The experiments were conducted with pre-treated wheat straw. After autoclaving the media components were mixed to a total volume of 200 mL. The fermentation was accomplished in 250 mL shaking flask. The cultivation flasks were inoculated by adding 40 mg of fungal pellet, gained from the pre-culture and incubated at 28°C and 150-190 rpm in a for 14 days in a shaker incubator (Certomat BS1).

Bioreactor fermentations 2L

The fermentation of the *T. reesei* strains was performed with Infors HT Labfors bioreactors. The fermentation was accomplished with M-media and a straw concentration of 14 g/L and 28 g/L dry weight. For inoculation, shaken flask pre-cultures as mentioned above were prepared, with the exception that incubation was only for 5 days.

Compressed air was used for oxygen supply. The oxygen concentration was set to 20-30 %. The stirrer was set to work in a range of 130-500 rpm. The oxygen supply and stirrer speed were controlled via a cascade.

2.3.4 Morphology analysis

The fungal hyphae were fixated by adding 10% (v/v) of a 10% (w/v) formaldehyde solution. The fixed samples were stored at 6 °C for future analyses.

Therefore the fixated samples were washed with millipore H₂O and with 50 mM C-buffer with a pH-value of 9.2. The washed samples were transferred to an object slide. As staining solution three different dyes were used. Firstly, the samples on the slides were incubated with Calcoflour white stain

for 5 min. The laser of the microscope was adjusted the excitation at 355 nm. The range of detection was 370 to 420 nm.

For the staining with acridine orange the staining solution was added to the Calcoflour white dye. The excitation wave length is at 488 nm and the detection at 530 ± 20 nm.

For staining with fluorescence brightener, a concentration of Calcoflour white of 0.001% was used. The samples were incubated for 5 min before measurement, which was carried out at 370 to 420 nm.

Septa analysis

The gained pictures from the CLSM were analyzed with a computer program which was developed by Petrasek Zdenek. The program is able to use the files from the CLSM which were saved in .lif format. The pictures are three dimensional and the program is able analyze across the z-axis. The septa could be tagged by clicking on it. The program calculates the distances between two tagged septa. Next the program calculates the thickness starting from the cell wall to the other site of the septa. As result, the coordinates of the setted points, the calculated length and the thickness of the septa, were saved as a .txt file.

2.3.5 Enzyme activity

Analysis of protein concentration

Protein content in the supernatant of fungal cultivation was measured with the Bradford method. Firstly, the samples were purified by precipitation. Therefore 400 μ L sample, 20 μ L Potassium phosphate and 20 μ L calcium chloride were mixed. After that 1 mL ethanol (1:2 diluted) was added. The solution was mixed for 1 min at 14000 rpm. The supernatant was discarded and the washing step with ethanol was repeated. The supernatant was discarded and 200 μ L of 5x staining RotiQuant (carl roth) undiluted solution was added and the pellet was resolved. Proteins were measured against BSA standards. The samples were measured as recommended by the manufacturer at 595 nm.

Measurement of beta-glucosidase activity

The samples were diluted appropriately. 250 μ L of p-NPG solution was pipetted in an Eppendorf tube and 250 μ L enzyme solution was added. The mixture was incubated for 10 min and 300 rpm at 50 °C in a Thermocycler. The reaction was stopped by adding 500 μ L of Na_2CO_3 and kept for 5 min on ice. Measurement was at 405 nm. As blank 250 μ L of p-NPG and 250 μ L Na-Ac was used. For calibration 8 dilutions of p-NP solution in a range of 0.05 mM to 1 mM were prepared. 250 μ L of diluted p-NP solutions and 250 μ L of Na_2CO_3 in an Eppendorf tube. The measurement was at 405 nm.

Measurement of Filter Paper Activity (FPA)

The FPA was determined according to the assay described by T.K. Ghose [19]. Each sample contained 1 mL 0.05 M Na-citrate buffer and 500 μ L diluted enzyme solution. For each concentration three samples were required. To two of the samples a filter paper strip was added, the other one was used as a blank. The samples were incubated at 50 °C for 60 min in 30 mL eprouvettes. Afterwards 3 mL DNS solution were added and the samples were boiled for exactly 5 min. The samples were diluted with 20 mL of water and cooled for 20 min on ice. To calculate the total enzyme activity a calibration was necessary. Therefore series of glucose solutions (2, 3.3, 5, 6.7 mg/mL) were prepared and 3 mL DNS solution was added. From that step onward the standards were treated the same way as the samples. For the calibration and the samples one additional blank was required. It contained 1.5 mL citrate buffer and was treated the same way as the samples. The measurement was conducted at 540 nm with a spectrophotometer.

Measurement of xylanase activity :

The determination of endo 1,4- β -xylanase activity was done according to the method, developed by Michael J. Bailey et al [20]. The enzyme solution was diluted with 50 mM Na-Citrate. 1.8 mL of Birchwood-xylan and 200 μ L of enzyme solution are filled in an eprouvette and incubated for 5 min at 50 °C. 3 mL of DNS solution was added and boiled for 5 min. The reaction mixture was cooled on ice and measured at 540 nm. The solution blank was treated like above but the enzyme solution was added after the incubation at 50 °C. For measurement a blank containing 1.8 mL of substrate and 200 μ L of Na-citrate was prepared. For calibration xylose standards in a range of 2-10 mmol/mL were used.

3 Results and Discussion

These methods were applied to find evidence for the correlation of the process conditions, morphology and enzyme production as mentioned above in 1.3. The size of septa and number of branches were determined and compared depending on inoculation method. The different experimental set-ups applied in this study are listed in Table 11.

Table 11: Description of Experiments conducted in this study

Experiment	Media	Strain	Inoculation	Conditions	Label
Experiment 1 (E1) without pre-culture	Lactose	QM9414	Agar	250 mL, 190 rpm, 28°C	QM-L-AG-E1
		QM9414	Spore	250 mL, 190 rpm, 28°C	QM-L-SP-E1
		Δ Cre	Agar	250 mL, 190 rpm, 28°C	Cre-L-AG-E1
		Δ Cre	Spore	250 mL, 190 rpm, 28°C	Cre-L-SP-E1
	Straw	QM9414	Agar	250 mL, 190 rpm, 28°C	QM-S-AG-E1
		QM9414	Spore	250 mL, 190 rpm, 28°C	QM-S-SP-E1
		Δ Cre	Agar	250 mL, 190 rpm, 28°C	Cre-S-AG-E1
		Δ Cre	Spore	250 mL, 190 rpm, 28°C	Cre-S-SP-E1
Experiment 2 (E2) with pre-culture	Lactose	QM9414	Agar	250 mL, 190 rpm, 28°C	QM-L-AG-E2
		QM9414	Spore	250 mL, 190 rpm, 28°C	QM-L-SP-E2
		Δ Cre	Agar	250 mL, 190 rpm, 28°C	Cre-L-AG-E2
		Δ Cre	Spore	250 mL, 190 rpm, 28°C	Cre-L-SP-E2
	Straw	QM9414	Agar	250 mL, 190 rpm, 28°C	QM-S-AG-E2
		QM9414	Spore	250 mL, 190 rpm, 28°C	QM-S-SP-E2
		Δ Cre	Agar	250 mL, 190 rpm, 28°C	Cre-S-AG-E2
		Δ Cre	Spore	250 mL, 190 rpm, 28°C	Cre-S-SP-E2
Experiment 3 (E3) with pre-culture	Lactose	QM9414	Agar	250 mL, 150 rpm, 28°C	QM-L-AG-E3
		QM9414	Spore	250 mL, 150 rpm, 28°C	QM-L-SP-E3
		Δ Cre	Agar	250 mL, 150 rpm, 28°C	Cre-L-AG-E3
		Δ Cre	Spore	250 mL, 150 rpm, 28°C	Cre-L-SP-E3
	Straw	QM9414	Agar	250 mL, 150 rpm, 28°C	QM-S-AG-E3
		QM9414	Spore	250 mL, 150 rpm, 28°C	QM-S-SP-E3
		Δ Cre	Agar	250 mL, 150 rpm, 28°C	Cre-S-AG-E3
		Δ Cre	Spore	250 mL, 150 rpm, 28°C	Cre-S-SP-E3
Experiment 4 (E4) with pre-culture	Straw	QM9414	Spore	2 L, 28°C	QM-S-SP-E4
		Δ Cre	Spore	2 L, 28°C	Cre-S-SP-E4
Experiment 5 (E5) with pre-culture	Straw	Δ Cre	Spore	2 L, 28°C	Cre-S-SP-E5

3.1 Optimization of analysis

Improvement of the staining method

Firstly, samples were stained with Calcofluor White stain which contains two different dyes, Calcofluor white and Evans blue. Calcofluor white is a non-specific fluorochrome that binds cellulose and chitin. Evans blue acts as a counterstain and diminishes background fluorescence [21]. The first experiment, E1 (Table 1), was accomplished with both fungal strains. As it can be seen in Figure 5, there was a remarkable difference in CLSM pictures taken after 8 and 14 days of incubation. Pictures from the 14th day of the fermentation were blurry and the septa were hardly distinguishable. Unspecific staining of secreted proteins and shell proteins from dead cells is a likely explanation. Non-specific reactions can occur when tissues samples are used.

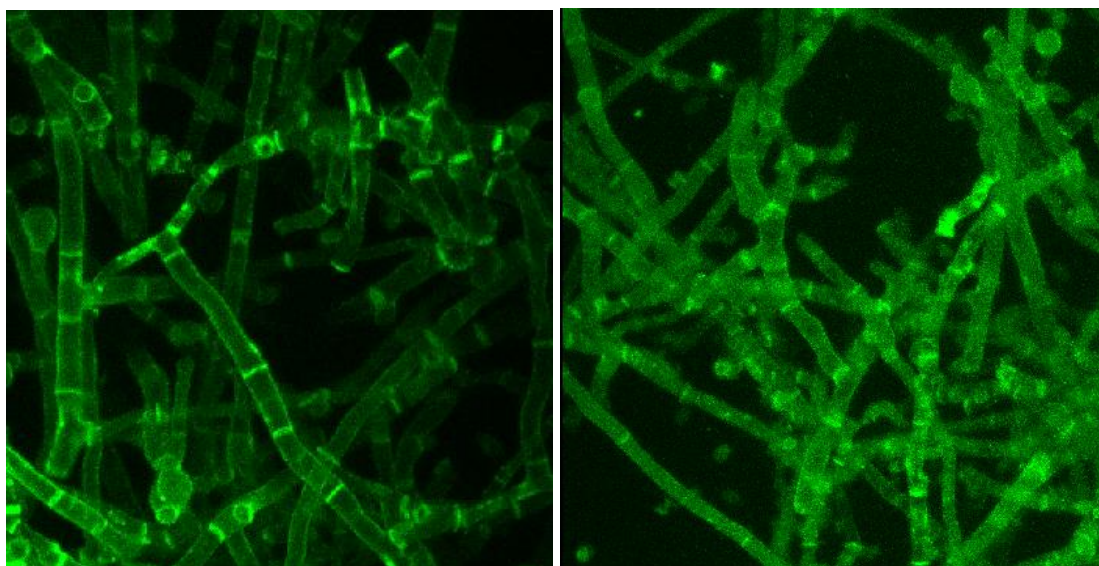


Figure 5: Left: Fermentation after 8 days; Right: Fermentation after 14 days.

To increase picture clarity Calcofluor without the addition of Evans blue was applied. The fluorescent brightener should only bind to chitin and cellulosic material. The result was an increase in sharpness of septa but the intensity of the picture was much lower. When the laser intensity was increased, the intensity was rising but the sharpness of the septa was decreased. As no improvement was achieved, Calcofluor white stain was used in further investigation.

Further investigation revealed, that the staining was more successful and the emitted light intensity was increased when the stained fungi was bound to straw. This may happen because more cellulolytic proteins are on the surface of the cells.

Increasing contrast

As it can be seen in Figure 6 Calcofluor white stain also binds to cellulose structures and the fungi was difficult to distinguish from the straw. To improve the analysis of the CLSM picture, the usage of a third dye which binds to the fungi should increase the fluorescent contrast. Acridine orange is a metachromatic dye which stains double stranded and single stranded nucleic acids. The dye emits green fluorescence upon excitation at 480-490 nm [22].

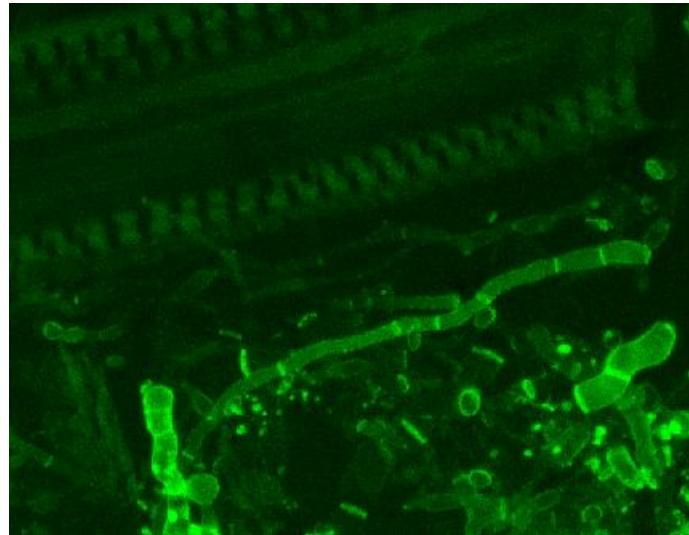


Figure 6: Calcofluor stain of straw and fungi

As it can be seen in Figure 6 the results the resolution was low. For staining acridine orange needs a different pH value than Calcofluor white stain. Based on the pH necessary to stain hyphae with Calcofluor (9.2), acridine orange did not improve the resolution of the CLSM picture as the pH necessary was 7.2. As a result, no difference was found between the samples with and without acridine orange. Based on the results mentioned above, Calcofluor white stain was chosen be the best staining dye and was used throughout the study.

3.2 Differences in morphology in dependence of fermentation conditions and strain

Experiment 1 – Fungal cultivations on lactose without pre-cultures

Firstly, shaken flasks cultivations without pre-cultures were accomplished (E1, Table 11). Cultivations were directly started by addition of fungi grown on agar and freshly harvested spores. A concentration of 10^5 spores was used to inoculate the culture, as it was done in the study of F.C. Domingues et al. [16].

The agar and spore inoculated fermentations could not be compared, because they were growing in different speed. In flasks inoculated with pieces of agar the fungi were growing much faster, reaching the end of the fermentation earlier. This is based on the higher biomass concentration in the beginning. For the spore cultures, the increase of biomass took more time. This is shown in Figure 7.

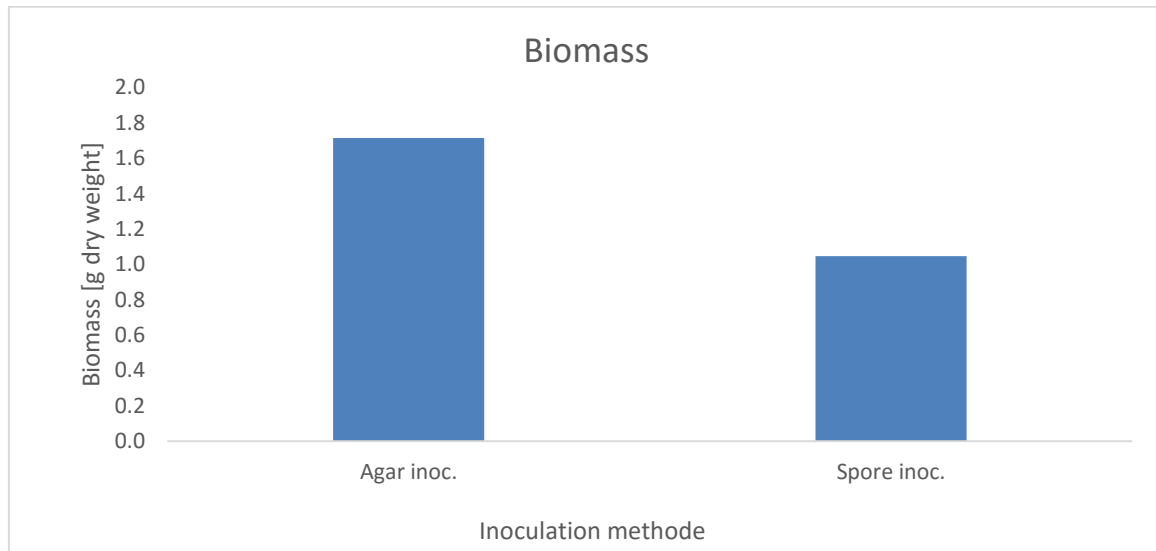


Figure 7: Biomass concentration after 8 days for Cre-L-AG-E1 and Cre-L-SP-E1

Further, the differences in growth development can be seen in the CLSM picture depicted in Figure 8. When comparing samples analysed after 2 days of fermentation (Figure 8, top left and the top right corner) the varieties can be clearly seen. Cre-L-AG-E1 shows long and thin cells and a low number of branches. The cell density was higher developed than of the spore inoculated culture shown in the top right picture. Cre-L-SP-E1 developed shorter cells and an increased number of branches. The cell density was lower.

After 8 days the pictures revealed that the fermentations, were in a different stage of development. On the 8th day Cre-L-AG-E1 (bottom left corner) already started to produce spores and growth peak was reached. The spore inoculated culture (bottom right corner, Cre-L-SP-E1) reveals an increased number of branches but no spores were produced.

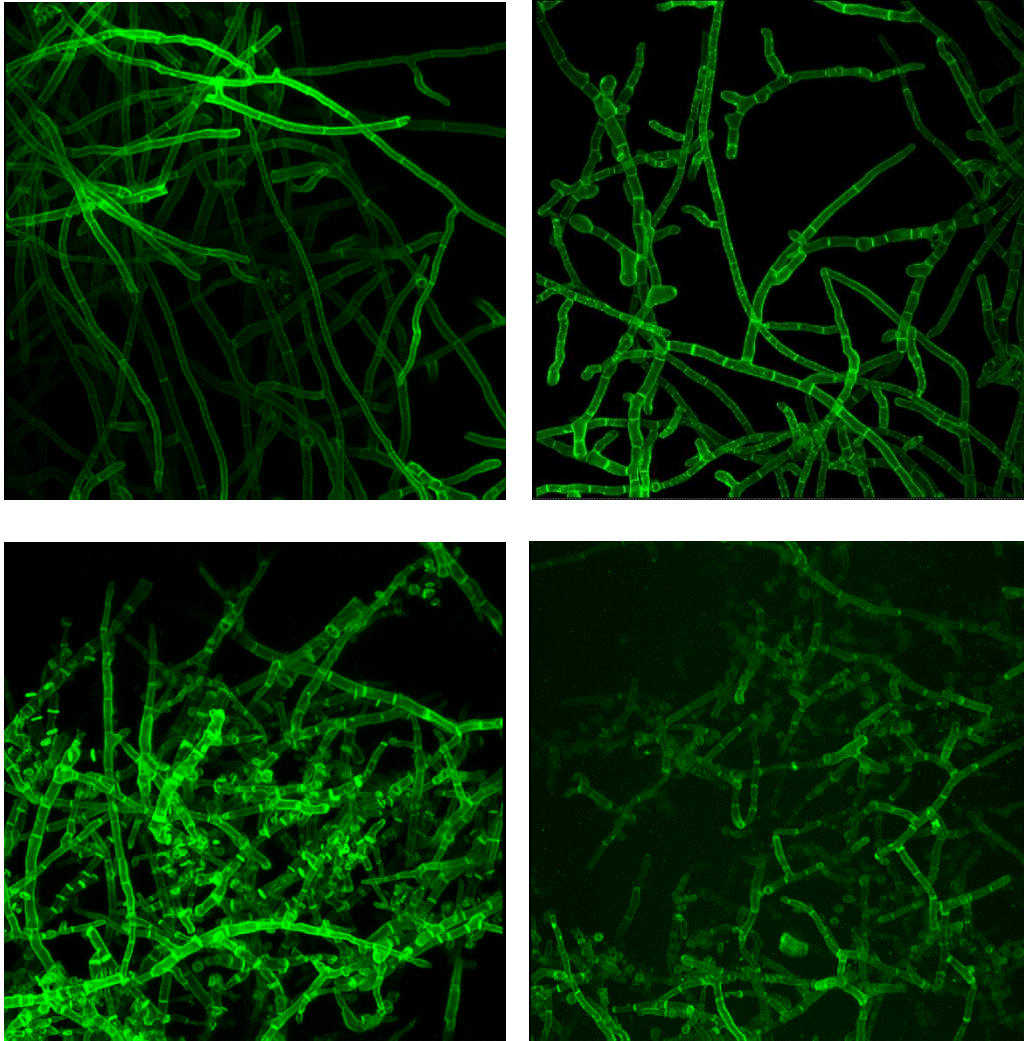


Figure 8: CLSM picture of lactose fermentations. Samples were taken after 2 and 8 days of fermentation. Top left: Cre-L-AG-E1 after 2 days; Top right: Cre-L-SP-E1 after 2 days; bottom left : Cre-L-AG-E1 after 8 days Bottom right: Cre-L-SP-E1 after 8 days

The spore inoculated fermentations were still slower. Further investigations revealed that they were in different stage of development after the same amount of time. As the spore inoculated cultures started to produce reasonable amounts of enzymes, the agar inoculated cultures were already reforming spores. The evaluation of the CSLM pictures showed it impossible to count enough septa to get a reliable analysis. The biomass concentration of the spore fermentations were too low after 8 days. As a result, the starting conditions had to be equalized.

Experiment 2 – Fungal cultivations on lactose with glucose pre-culture

To render comparison of different cultivation conditions possible, glucose pre-cultures were prepared (E2, Table 11). Both strains were grown for 2 days in glucose based M-media and 40 mg of the fungal biomass were added as inoculum. To investigate the change of fungi growth lactose as C-source was used. The first change of the fermentation was visible to the unaided eye.

As it can be seen in Figure 9 the macromorphology of the cultivations started with spores and with agar differed significantly. Figure 9 clearly reveals the macroscopic differences. The flasks inoculated with agar pieces showed floating and growing pellets in the media after 24 h. As the fermentation was going on the pellets grew bigger and after 3 days the single pellets were impossible to distinguish. The fermentation media with spores was blurry after the same time. When the growth went on the media changed and a highly viscous solution was obtained after 3 days.



Figure 9: Fermentation with lactose as C-source after 24 h inoculated with pre-culture; Left: Inoculation with agar piece; Right: Inoculation with spore

To determine fungal growth, biomass was harvested and weighted after 336 h of fermentation. As the biomass concentrations were similar for both experimental set ups was equal. Since the starting conditions were the same as well, fungal growth rates were assumed to be equal. These first results of the lactose shaking flasks showed similar results than F.C. Domnigues et al., which proposed, that a high spore concentration leads to filamentous mycelium and a low concentration of pellets. These differences made it clear that the kind of inoculation could change the macromorphology.

To analyse the impact of inoculation method on the micromorphologie, experiments (E1, Table XYZ) were also analysed by CLSM. With the self-developed computer program, the CLSM pictures were examined and the length of the septa were determined. It has been previously described that the volume and the number of branches in fermentation with filamentous fungi can be utilized as base of comparison of different fermentation conditions [ref]. To render reliable analysis possible, 100 septa were counted per image. The pre-culture increased the cell density making it possible to compare the two inoculation methods. As it can be seen in Figure 8, lactose grown cultures were growing in long and thin septa as compared to straw cultures which developed in shorter and thicker septa. Results shown in Figure 12 support this outcome. Independent of strain, the agar inoculated cultures showed longer septa while spores inoculated cultures were shorter.

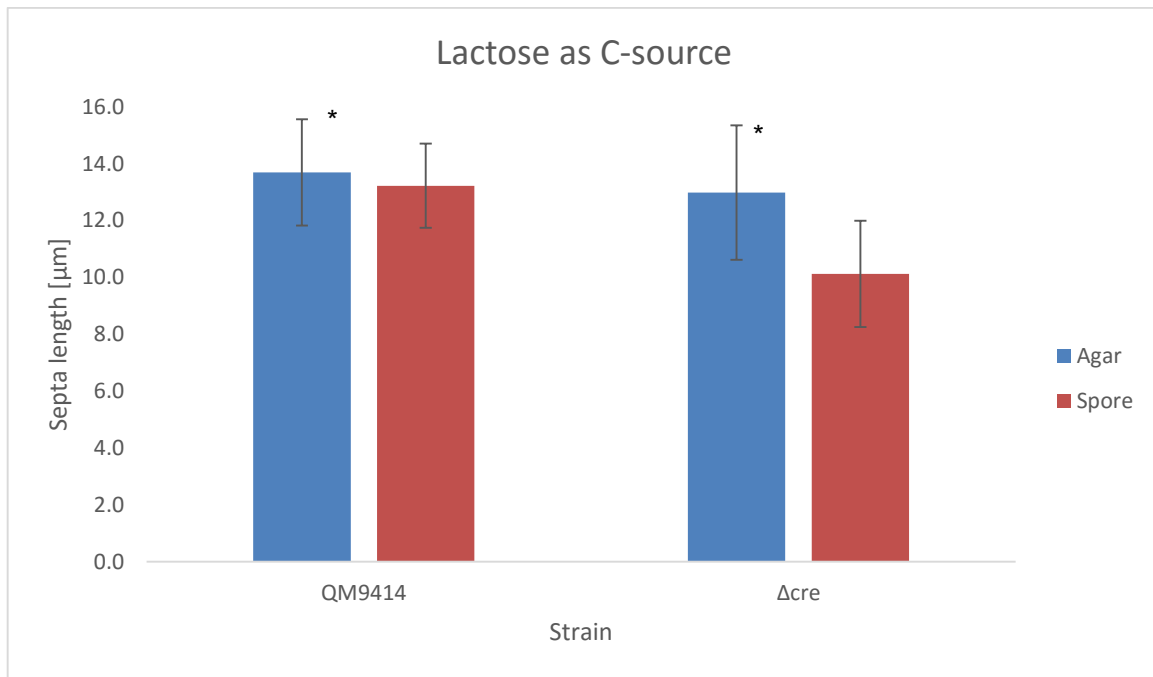


Figure 10: Comparison of average septa length of QM-L-AG-E2, QM-L-SP-E2, Cre-L-AG-E2 and Cre-L-SP-E2

Independent of inoculation, QM9414 developed longer septa in average than ΔCre . The difference between the inoculation methods was 28% for ΔCre , while QM9414 showed nearly the same results.

As mentioned above, the experiments were accomplished with straw as C-source, according to its industrial importance [23]. The influence of the substrate on the morphology is important to investigate, as the morphology may also have influence on the enzyme production.

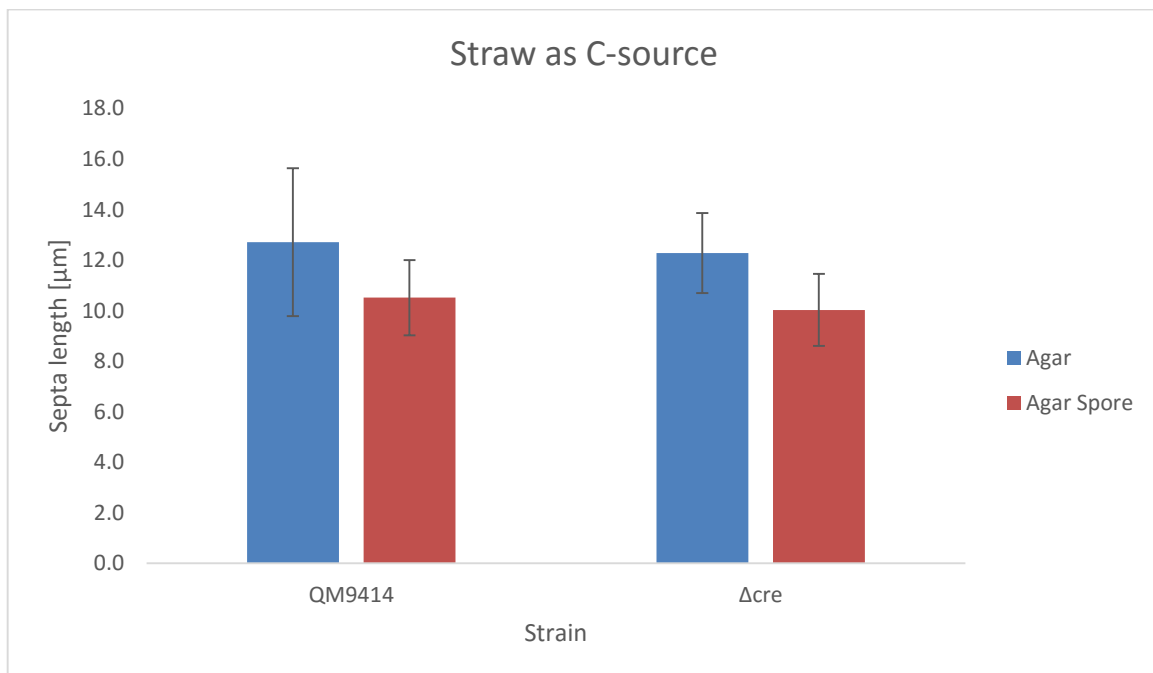


Figure 11: Comparison of average septa length of QM-SL-AG-E2, QM-S-SP-E2, Cre-S-AG-E2 and Cre-S-SP-E2

The straw fermentations lead to a decrease of the average length for both strains as compared to the lactose cultures. The average difference between agar and spore inoculations was about 21%. Both

straw and lactose experiments were inoculated with the same amount of spores and the samples were taken after 8 days. In Figure 12 the difference between lactose and straw cultures is shown. The left picture shows that agar inoculated lactose fermentations lead to long and thin septa while in the right picture straw resulted in smaller and thicker septa. The cell density was increased as well. This result was similar with QM9414 and Δ Cre.

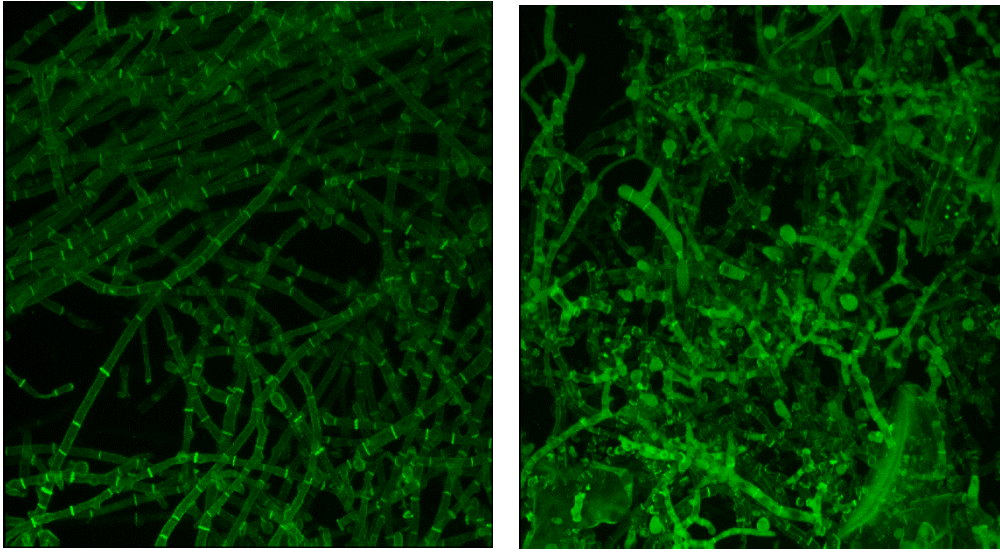


Figure 12: Left picture: QM-L-AG-E2; Right picture: QM-S-AG-E2

To summarize the results, the strains differ in their average septa length under both cultivation conditions (lactose and straw cultures) presented. Δ Cre developed shorter cells while the average length of QM9414 was higher. When grown on straw, both QM9414 and Δ Cre, developed a higher differentiation of the average length between agar and spore. Both strains develop thicker septa, when length is decreased.

Experiment 3 – Influence of agitation velocity on fungal morphology

To further investigate the influence of process conditions on the fungal morphology the shaking speed was decreased to 150 rpm (E3, Table 1). The samples of E3 were taken after 8 days and analysed with CSLM and the self-developed computer program.

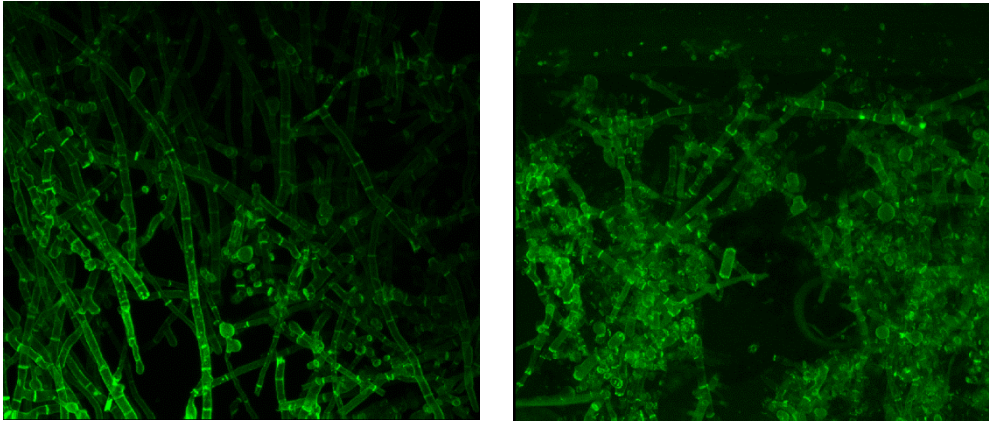


Figure 13: Fermentation with reduced shaking speed. Left picture: QM-L-AG-E3; Right picture: QM-S-AG-E3

As it can be seen in Figure 13 and Figure 14, a reduced shaking velocity resulted in thicker and shorter cells, as compared to fermentation agitated with 190 rpm, independent of C-source and inoculation method (e.g. Figure 12).

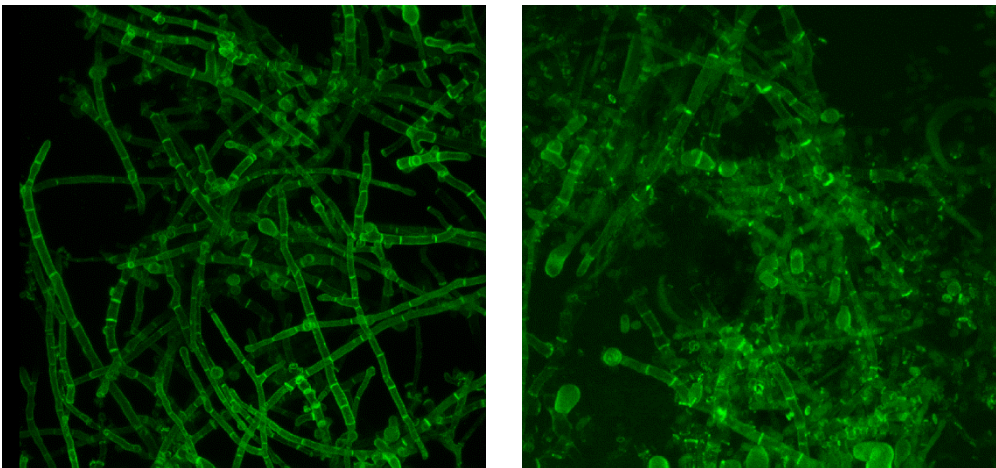


Figure 14: Fermentation with reduced shaking speed. Left picture: QM-L-SP-E3; Right picture: QM-S-SP-E3

However, Figure 14 reveals the difference of lactose and straw fermentations. As the average length of the spore septa was already shorter, the average length did not seem to be significant different, but the thickness was increased. The measured septa length is depicted in Figure 15.

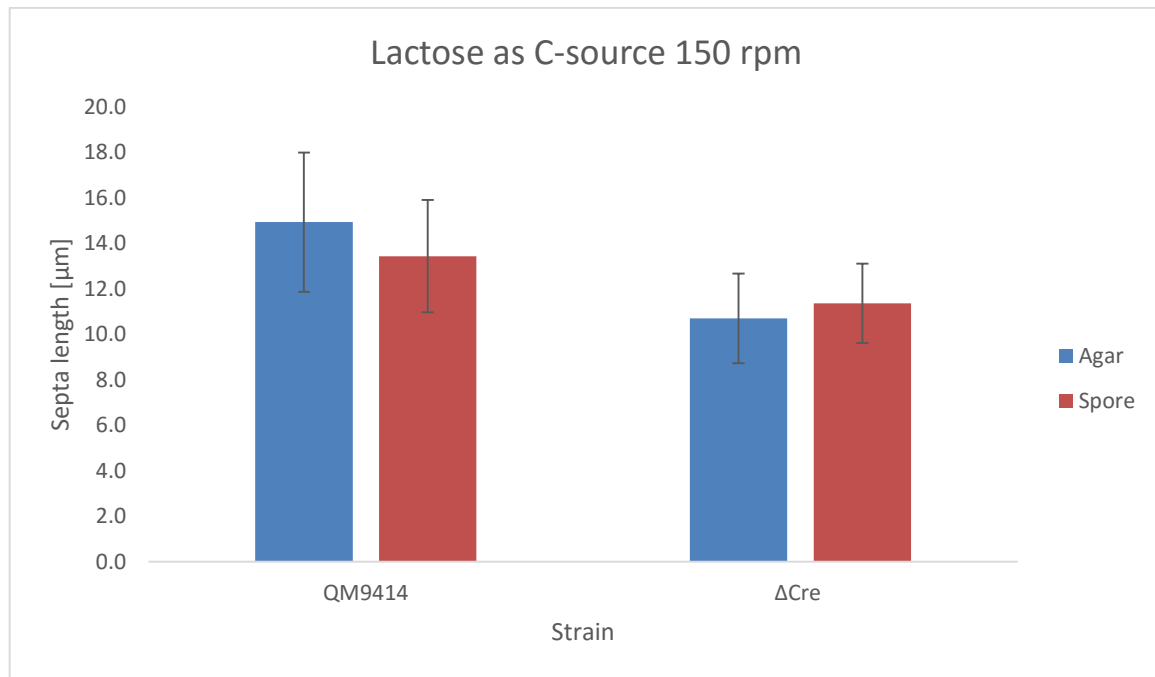


Figure 15: Comparison of QM-L-AG-E3, QM-L-SP-E3, Cre-L-AG-E3 and Cre-L-SP-E3

The same experiments and comparison was done with fermentations, conducted with straw as C-source. The results of the cultures with straw as C-source, were shown in Figure 16.

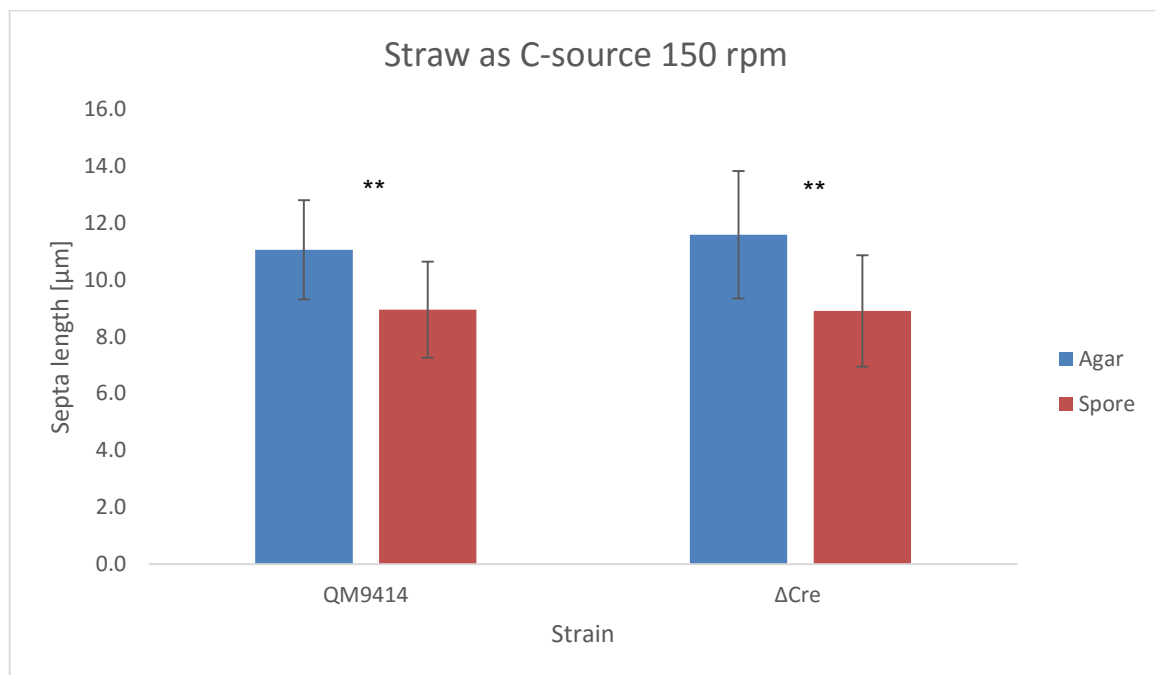


Figure 16: Comparison of QM-S-AG-E3, QM-S-SP-E3, Cre-S-AG-E3 and Cre-S-SP-E3

The reduction of shaking speed did influence the morphology by decreasing the average length. Comparing QM9414 and Δ Cre, the results were the same. Both strains showed a progression to develop shorter septa independent from the inoculation method. Spores still grow shorter septa. The

average length of the cells was decreased compared with the 190 rpm fermentation. The number of branches did not differ compared with the first experiment. In all experiments QM9414 showed to develop longer, while ΔCre developed shorter cells.

The results gained from the comparison in Figure 15 and Figure 16 initiated the investigation of the thickness and the number of branches of the cells. The correlation of length and thickness is shown in Figure 17. Independent of the fungal strain, the thickness is increased when shorter cells are formed. The average thickness of agar inoculated culture cells was between 3.0-3.3 μm and spore inoculated cultures ranged from 3.1-4.7 μm . As the shaking speed was decreased to 150 rpm, there was hardly any difference of cell thickness between agar and spore inoculation (Figure 18). The average length decreased and the average thickness was increased, independent from strain or inoculum.

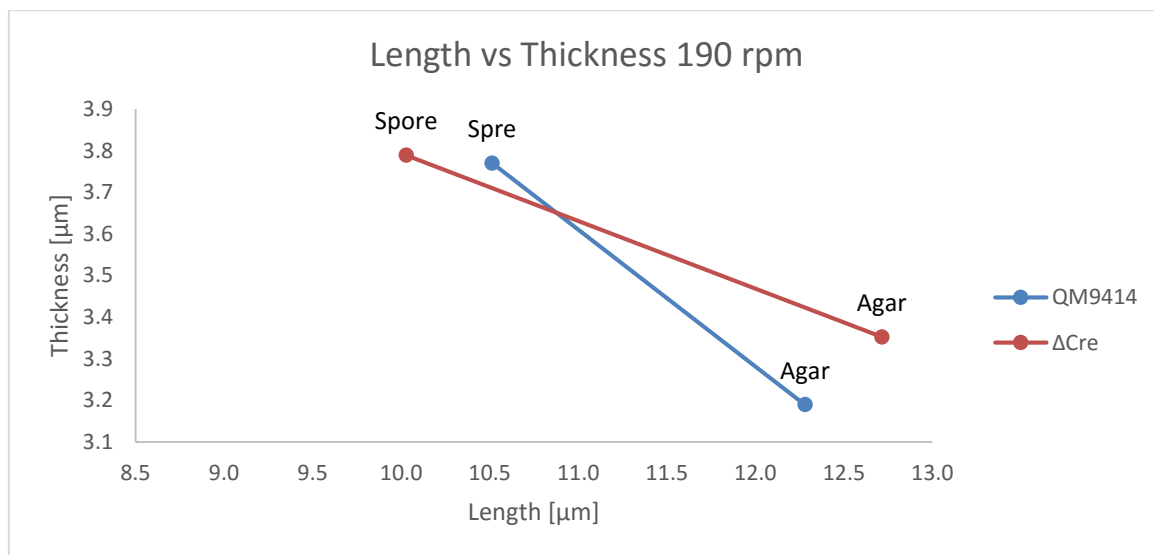


Figure 17: Length vs thickness at 190 rpm straw

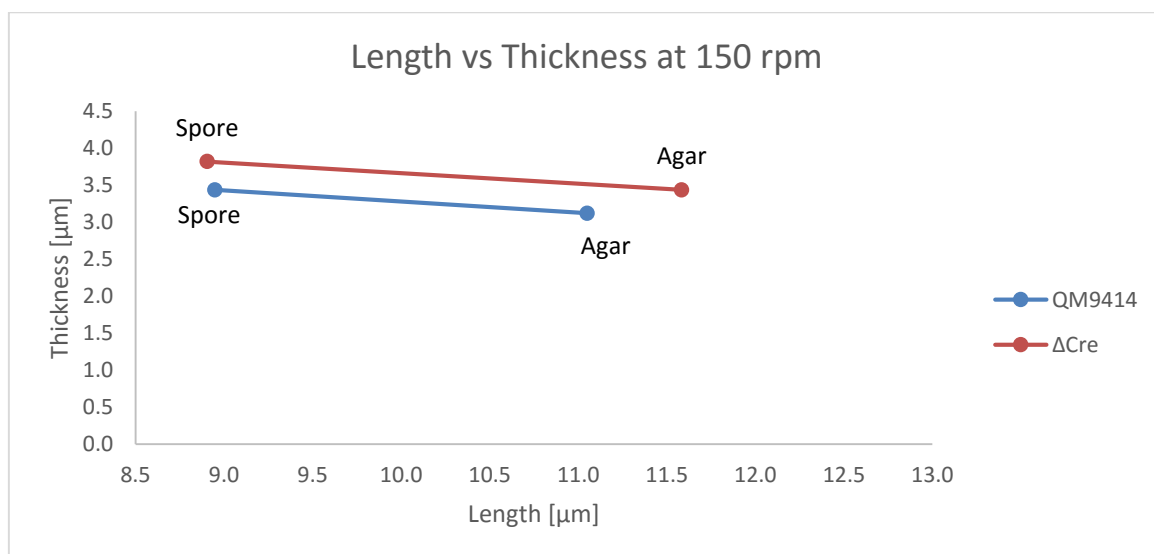


Figure 18: Length vs thickness at 150 rpm straw

As it can be seen in Figure 17 and Figure 18, change in shaking speed lead to a significant change of morphology. The average thickness of agar inoculated culture cells was between 3.0-3.3 μm and spore inoculated cultures ranged from 3.1-4.7 μm . As the shaking speed was decreased to 150 rpm, there was hardly any difference of cell thickness between agar and spore inoculation. The average length decreased and the average thickness was increased, independent from strain or inoculum. Slower shaking speed leads to lower nutrient and oxygen dispersion. It was suggested that the oxygen supply had a major impact on the development of the morphology.

Experiment 4 – Fermentation in 2 L bioreactor

To further investigate the influence of process-conditions on the morphology, in E4 the experiments were up scaled to 2 L working volume. A change from shaken flask to bioreactor cultivations represents significant changes in process conditions. The oxygen supply was limited to the surface area while in the bioreactor the oxygen level was controlled online with a stirrer speed and aeration cascade. During cell growth the demand of oxygen as well as the media viscosity changes over time. Monitoring and controlling pO_2 in high solid state fermentations with filamentous fungi was challenging as the media clogged the oxygen-prob, resulting in massive diffusion limitations from the bulk to the probe, rendering online measurement difficult. This resulted in fluctuating oxygen levels and oscillating stirrer speeds, leading to different shear-stresses and therefore in changing growth conditions.

Based on the favourable results in shaken flask cultivations (E2 and E3, Table 1), bioreactor fermentations were inoculated with spores. The experiment should reveal the influence of the upscale on cells morphology. After 8 days the samples were analysed. The results were similar to the small scale experiments. QM9414 developed longer and thinner septa than the ΔCre mutant.

Summarizing the results, spore inoculation always results in shorter septa than agar inoculation. An interesting correlation was determined. Shorter septa showed also thicker septa. The average length of agar inoculated septa was between 11 to 17 μm compared to 7 to 12 μm of spore inoculation. The comparison of the strains revealed that QM9414 develops longer septa than ΔCre , independent of inoculation method. The number of branches was similar in all experiments. In total more branches were produced when spores were used as inoculation as compared to agar inoculated fermentations. This was independent of the fermentation conditions.

3.3 Fungal morphology influences the level of enzyme secretion by *T. reesei* strains

As mentioned at 1.3, the investigated theory was, that the process conditions influence the morphology. The next step of the investigation was to find evidence if the change in morphology influences the cellulase expression. Experiment E1 to E4 have proven that a change of process

conditions has a major impact on the morphology. A. Ahamed et al., report that most of the enzyme is secreted during tip growth and Wongwicharn et al., described evidence for an increased secretion of hen egg white lysozyme, in the presents of a higher number of branches [17].

If the assumption is correct, a higher enzyme activity is more likely when spores are used for inoculation, since this method showed a higher degree of branching in the CLSM analyses. As the biomass concentration of agar and spore inoculated cultures were the same, it was assumed, that the difference in enzyme concentration can be connected to a change in morphology.

The cellulase activity was used as key parameter of the study. It was used for comparison for any difference in enzyme production when the morphology was altered. Firstly FPA was related to the average septa length. The first examination was accomplished with the fermentation at 190 rpm. These results can be seen in Figure 19. It reveals that the cellulase activity was higher when the average cell length was decreased. This result was valid for both fungal strains.

The highest enzyme activity was reached with spore inoculation. In accordance with the previous results, spores develop shorter septa then agar inoculation [6]. This is in good agreement with these results, as the decrease in total cell length, resulted in a higher total cell number.

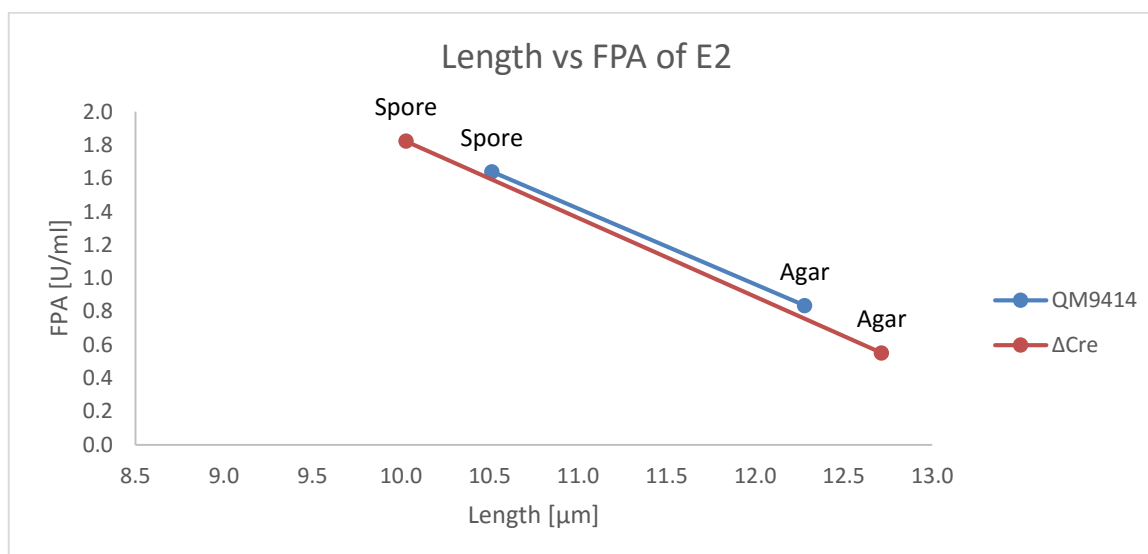


Figure 19: Length vs FPA at 190 rpm; Straw as C-source; QM9414 and ΔCre

Assuming that shorter septa indicates a higher enzyme production, the enzyme activity may be increased at 150 rpm as previous results showed a decreased average septa length at this shaking speed (E3, Tabelle 11). The activity measurement revealed an increase in cellulase production of the agar inoculated fermentations, while the spore inoculated fermentations showed nearly the same activities (Figure 20).

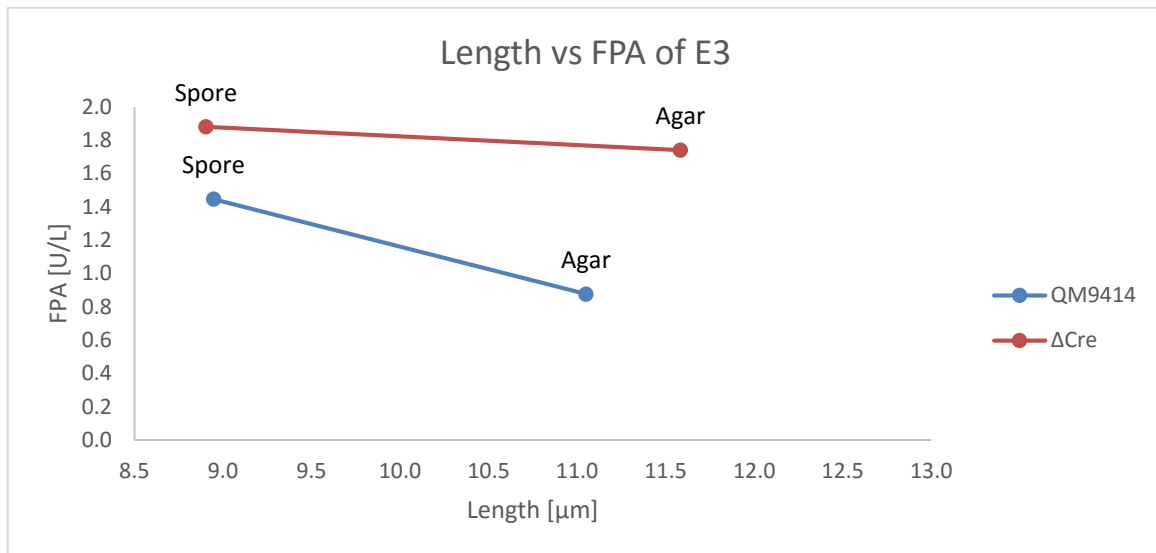


Figure 20: Length vs FPA at 150 rpm; Straw as C-source; QM9414 and Δ Cre

The comparison showed, that at 150 rpm the differences in average cell length seem to have less influence on FPA than at 190 rpm. Therefore we took investigations one step further and related the cell thickness to the enzyme activity. The results of these experiments can be seen in Figure 21 and Figure 22. An increased FPA activity correlates with an increase in thickness.

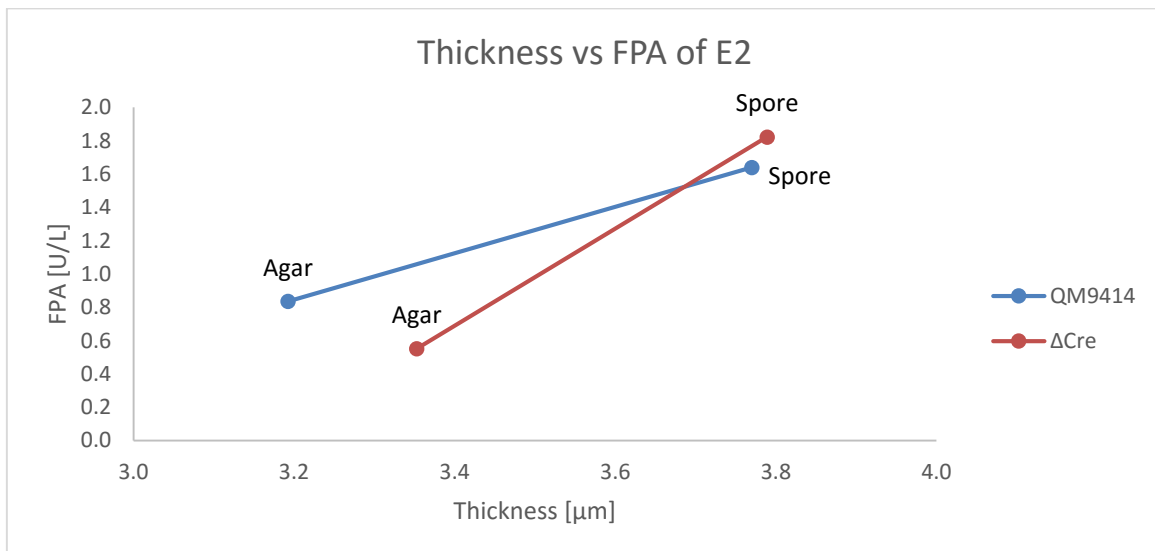


Figure 21: Thickness vs FPA 190 rpm; Straw as C-source; QM9414 and Δ Cre

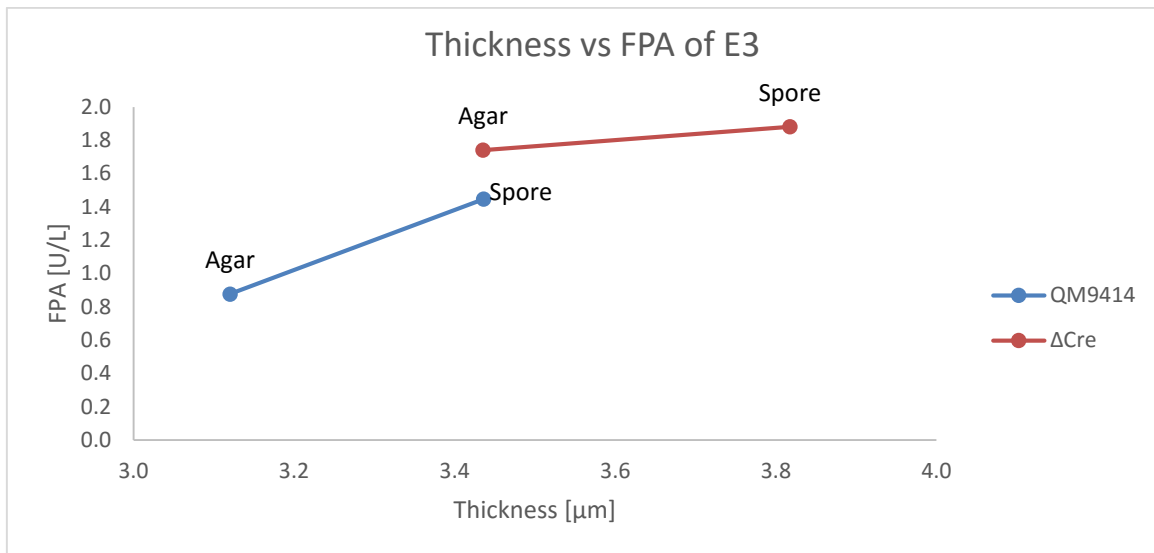


Figure 22: Thickness vs FPA 150 rpm; Straw as C-source; QM9414 and ΔCre

As Figure 21 and Figure 22 revealed, an increase of FPA activity seems to accord with an increase of the average thickness of the hyphae.

Based on the obtained results we draw the conclusion that it might be possible to influence the septa length by adjusting the cultivation conditions. Thus, shorter septa could be created yielding in a higher enzyme yield. To confere these results, other enzyme activities were measured. As the FPA assay is limited do its high detection limit and to the fact that it can only determine total enzyme activities, the investigation was extended to protein concentration, beta-glucosidase activity and xylanase activity. As it can be seen in Figure 23, the xylanase activity is higher when spores are used. For QM9414 the xylanase activity was 16 % higher.

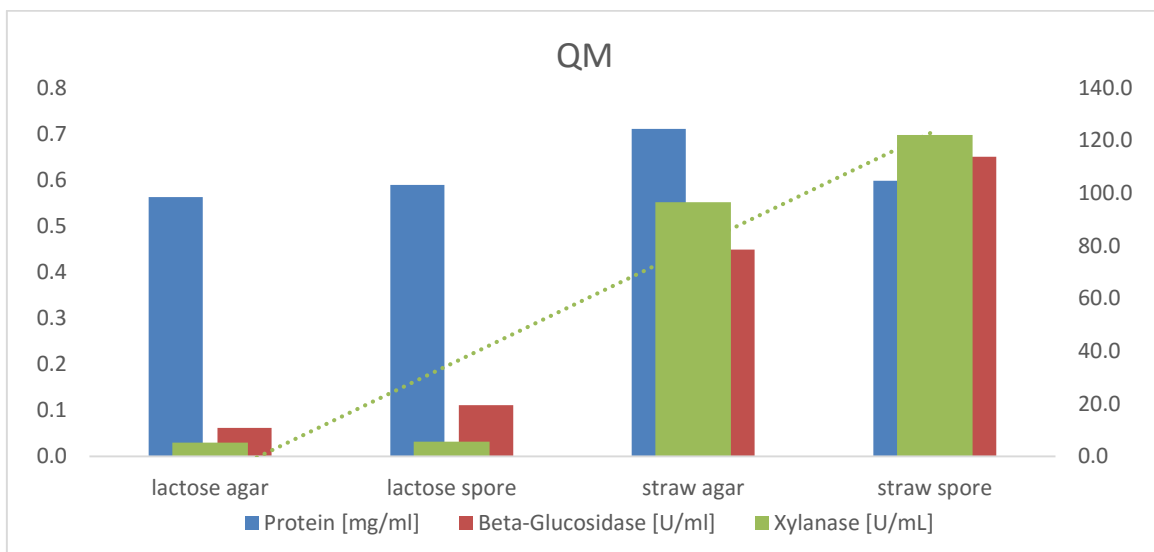


Figure 23: Protein concentration, beta-Glucosidase and xylanase activity of QM9414 of E2

The same results were obtained for Δ Cre (Figure 24) as the xylanase activity was 22 % higher.

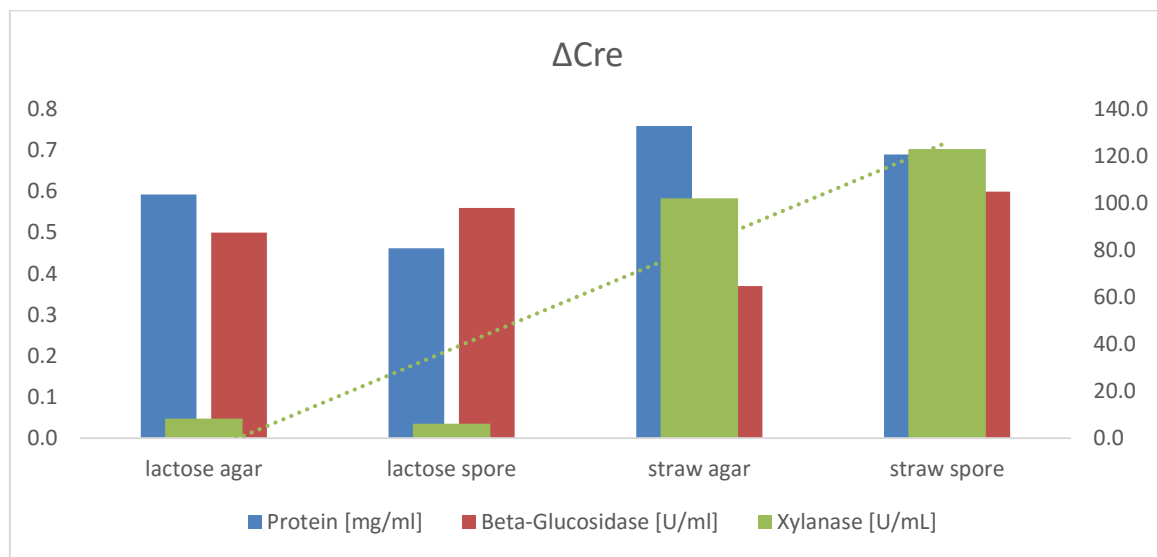


Figure 24: Protein concentration, beta-Glucosidase and xylanase activity of Δ Cre of E2

Similar results were observed when the fermentation were accomplished with 150 rpm. The detailed analysis of the 150 rpm fermentation can be found in the appendix in Figure 28 and Figure 29.

Scale up

When the volume of the fermentation (E4, Table 11) was scaled up to the results for protein concentration, xylanase and beta-glucosidase activities were similar, but the FPA activity were much lower. This was unexpected as the fermentation starting conditions and the media composition were the same. The first assumption was, that there is a difference in morphology that could explain the decrease. But the CLSM picture evaluation showed, that the overall size of septa did not change compared with the other fermentations. The results were shown in Figure 25.

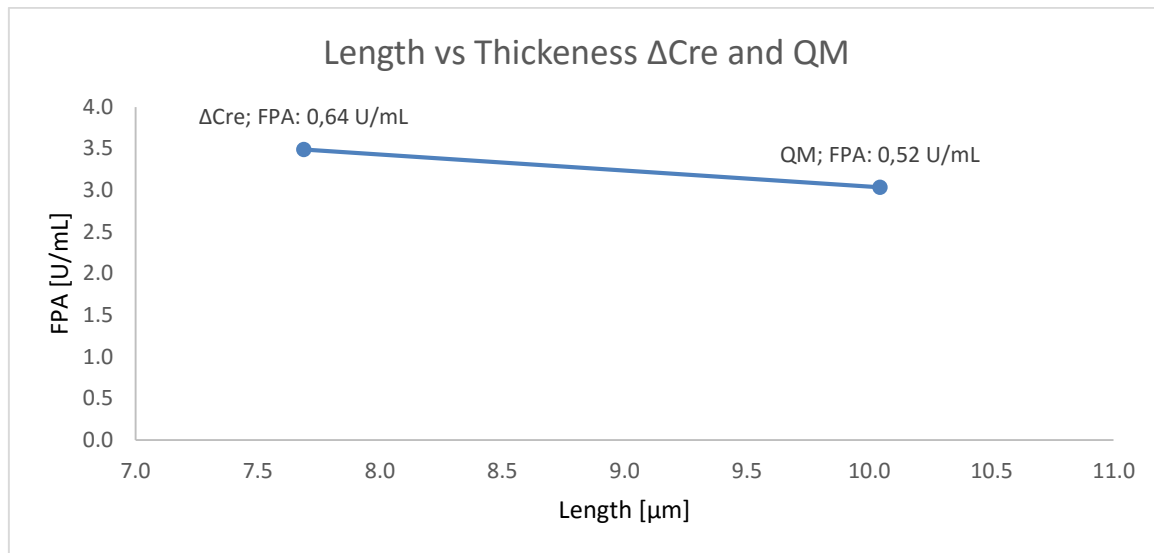


Figure 25: Length vs Thickness, 2L bioreactor, spore inoculation

The average thickness and length of E4 measured, could be assumed to be the same as E2 and E3 (Table 11). Compared with the highest shaking flask FPA, QM only achieved 36 % of the FPA and ΔCre 34% while the protein concentration, beta-glucosidase-activity and xylanase activity higher as shown in Figure 26.

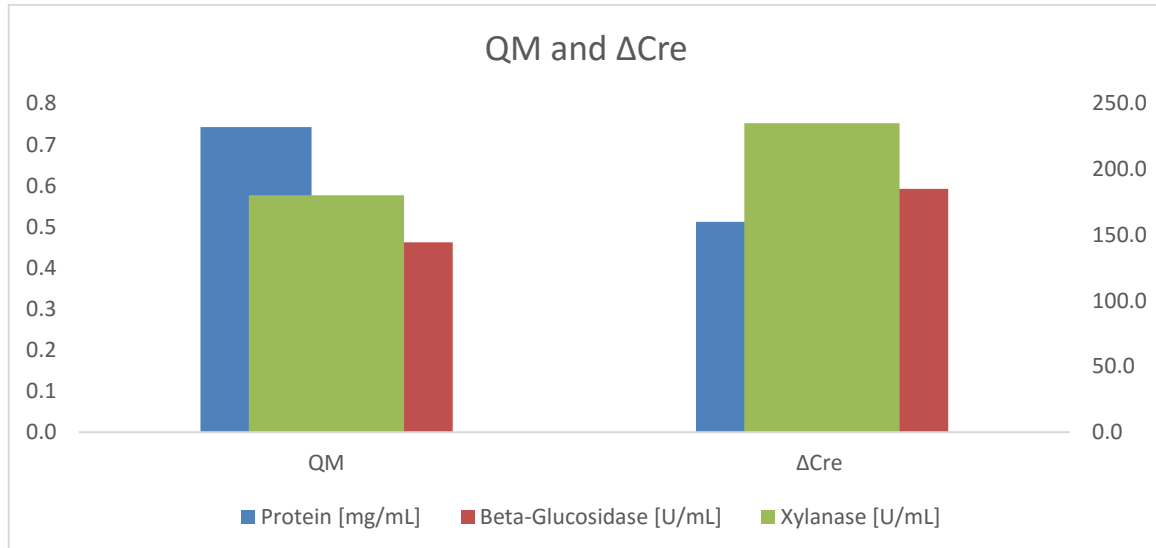


Figure 26: Determination of Protein concentration, beta-Glucosidase activity and xylanase activity at 2 L bioreactor of QM9414

The other reasons for the significant loss of activity could be the process monitoring and regulation problems mentioned in 3.2. Therefore the stirrer speed was increased (E5, Table 11) and better results were achieved. The total FPA activities were similar to the results of E2 (Table 11). FPA activity of ΔCre reached 1.31 U/mL while the FPA of QM9414 was at 1.2 U/mL. The results of the septa

morphology were similar as observed in the previous bioreactor experiments. Δ Cre developed shorter and thicker septa than QM9414 and the average size was the same as compared to E2.

4 Conclusion

This study showed, that there is a connection between process conditions, morphology and cellulose production in *T. reesei*. Changing one parameter, results in an alteration of the others. The results shown in 3, clarified the interactions shown in Figure 25.

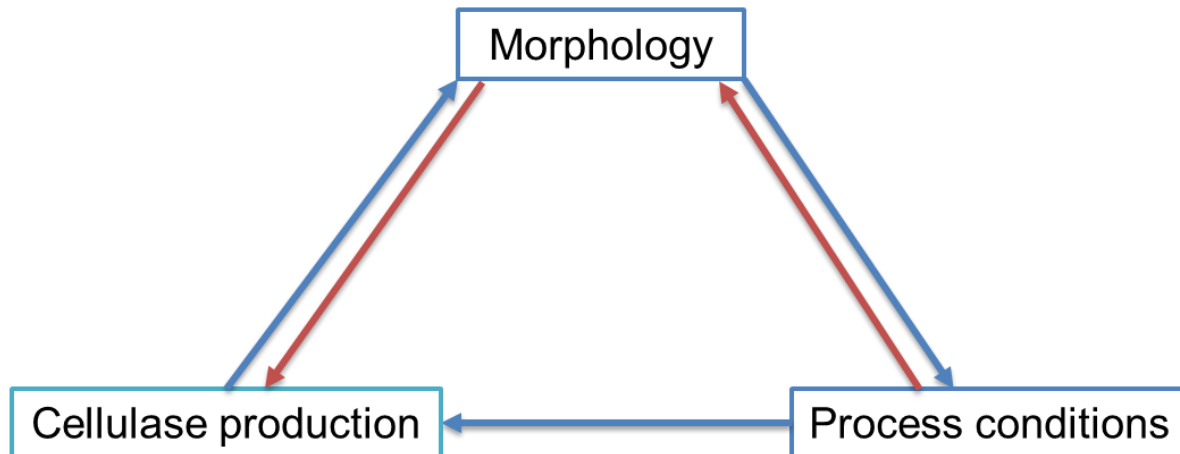


Figure 27: Relationship between process conditions, morphology and cellulase production

Process conditions

The influence of process conditions such as shaking speed, process condition and inoculation method on morphology and cellulase production were investigated. The inoculation method had a major impact on the morphology. This is in accordance with the findings of F. Domnigues et al. The spore inoculated experiments, developed shorter and thicker cells than agar inoculated cultures. The spore cultures grew in a higher disperse form, while agar experiments seemed to develop a more clumped form. This was the same for strain QM9414 and Δ Cre.

The change in process conditions resulted also in a change in morphology. If the shaking speed was decreased both QM9414 and Δ Cre developed shorter and thicker septa. This was independent from the inoculation method, while cultures gained through spore inoculation grew smaller cells compared with agar inoculated cultures. The results indicate that a reduced septa length correlates with an increased thickness of the cells.

Morphology

F. Domnigues et al, proposed, that the number of spores have a major impact on the culture development, which is in accordance with the results of this study [16]. Using spores instead of fungi grown on agar pieces, resulted in a dispersed growth of the fungi.

The reduced length of septa and the increased thickness, seem to influence the enzyme production positively since higher activities were detected independent on fungal strain or C-source. Therefore it can be assumed that shorter septa result in a higher enzyme production.

Regarding the hypothesis stated in chapter 1.3 the outcome of the performed experiments were interesting. Process conditions influence the morphology development, while the morphology has an impact on the cellulase production. A higher cellulase production could result in better growth conditions for the fungi as well as in a decrease of production cost. A higher cellulase concentration may also reduce the time needed for the saccharification of the lignocellulolytic feedstock. The correct combination of process-conditions and morphology lead to a higher enzyme production.

5 Literature

- [1] Y. Lin and S. Tanaka, "Ethanol fermentation from biomass resources: Current state and prospects," *Appl. Microbiol. Biotechnol.*, vol. 69, no. 6, pp. 627–642, 2006.
- [2] P. Kaparaju, M. Serrano, A. B. Thomsen, P. Kongjan, and I. Angelidaki, "Bioethanol, biohydrogen and biogas production from wheat straw in a biorefinery concept," *Bioresour. Technol.*, vol. 100, no. 9, pp. 2562–2568, 2009.
- [3] M. Dashtban, H. Schraft, and W. Qin, "Fungal bioconversion of lignocellulosic residues; Opportunities & perspectives," *Int. J. Biol. Sci.*, vol. 5, no. 6, pp. 578–595, 2009.
- [4] S. N. Naik, V. V. Goud, P. K. Rout, and A. K. Dalai, "Production of first and second generation biofuels: A comprehensive review," *Renew. Sustain. Energy Rev.*, vol. 14, no. 2, pp. 578–597, 2010.
- [5] B. Seiboth, C. Ivanova, and V. Seidl-seiboth, "Trichoderma reesei : A Fungal Enzyme Producer for Cellulosic Biofuels," *Intechopen*, pp. 309–341, 2011.
- [6] A. Ahamed and P. Vermette, "Effect of culture medium composition on Trichoderma reesei's morphology and cellulase production," *Bioresour. Technol.*, vol. 100, no. 23, pp. 5979–5987, 2009.
- [7] S. Bhargava, M. P. Nandakumar, A. Roy, K. S. Wenger, and M. R. Marten, "Pulsed feeding during fed-batch fungal fermentation leads to reduced viscosity without detrimentally affecting protein expression.," *Biotechnol. Bioeng.*, vol. 81, no. 3, pp. 341–7, Feb. 2003.
- [8] M. Mandels, J. Weber, and R. Parizek, "Enhanced cellulase production by a mutant of Trichoderma viride.," *Appl. Microbiol.*, vol. 21, no. 1, pp. 152–4, Jan. 1971.
- [9] R. Lejeune, J. Nielsen, and G. V. Baron, "Morphology of Trichoderma reesei QM 9414 in submerged cultures," *Biotechnol. Bioeng.*, vol. 47, no. 5, pp. 609–615, 1995.
- [10] T. Portnoy, A. Margeot, R. Linke, L. Atanasova, E. Fekete, E. Sándor, L. Hartl, L. Karaffa, I. S. Druzhinina, B. Seiboth, S. Le Crom, and C. P. Kubicek, "The CRE1 carbon catabolite repressor of the fungus Trichoderma reesei: a master regulator of carbon assimilation.," *BMC Genomics*, vol. 12, no. 1, p. 269, 2011.
- [11] V. Lecault, N. Patel, and J. Thibault, "Morphological characterization and viability assessment of Trichoderma reesei by image analysis.," *Biotechnol. Prog.*, vol. 23, no. 3, pp. 734–740, 2007.
- [12] M. Papagianni, "Fungal morphology and metabolite production in submerged mycelial processes," *Biotechnol. Adv.*, vol. 22, no. 3, pp. 189–259, 2004.
- [13] P. Ji., "Kinetics of filamentous growth and branching," *Grow. dungus*, 1995.
- [14] T. Wucherpfennig, K. a. Kiep, H. Driouch, C. Wittmann, and R. Krull, *Morphology and rheology in filamentous cultivations*, 1st ed., vol. 72, no. C. Elsevier Inc., 2010.

- [15] S. P. Booking, M. G. Wiebe, G. D. Robson, K. Hansen, L. H. Christiansen, and A. P. J. Trinci, "Effect of branch frequency in *Aspergillus oryzae* on protein secretion and culture viscosity," *Biotechnol. Bioeng.*, vol. 65, no. 6, pp. 638–648, 1999.
- [16] F. C. Domnigues, J. a. Queiroz, J. M. S. Cabral, and L. P. Fonseca, "The influence of culture conditions on mycelial structure and cellulose production by *Trichoderma reesei* Rut C-30," *Enzym. Microb. Technol.*, vol. 26, pp. 394–401, 2000.
- [17] a. Wongwicharn, B. McNeil, and L. M. Harvey, "Heterologous protein secretion and fungal morphology in chemostat cultures of a recombinant *Aspergillus niger* (B1-D)," *Enzyme Microb. Technol.*, vol. 24, no. 8–9, pp. 489–497, 1999.
- [18] R. Doppelbauer, H. Esterbauer, W. Steiner, R. M. Lafferty, and H. Steinmüller, "The use of lignocellulosic wastes for production of cellulase by *Trichoderma reesei*," *Appl. Microbiol. Biotechnol.*, vol. 26, no. 5, Aug. 1987.
- [19] I. Union, O. F. Pure, and A. Chemistry, "International Union of Pure Commission on Biotechnology * Measurement of," *Pure Appl. Chem.*, vol. 59, no. 2, pp. 257–268, 1987.
- [20] M. J. Bailey, P. Biely, and K. Poutanen, "Interlaboratory testing of methods for assay of xylanase activity," *J. Biotechnol.*, vol. 23, no. 3, pp. 257–270, 1992.
- [21] F. Analytical, "18909 Calcofluor White Stain," vol. 7, no. 1998, p. 18909, 2003.
- [22] I. Nicoletti and R. Mannucci, "Fluorescence microscopy analysis of nuclear alterations during apoptosis," pp. 7–9.
- [23] V. Novy, K. Longus, and B. Nidetzky, "From wheat straw to bioethanol: integrative analysis of a separate hydrolysis and co-fermentation process with implemented enzyme production," *Biotechnol. Biofuels*, vol. 8, no. 1, pp. 1–12, 2015.

List of figures

Figure 1: Cellulose degrading system of <i>T. reesei</i>	3
Figure 2: Growing mycelium with several tips	4
Figure 3 Aggregation model for coagulation filamentous microorganisms [14]	4
Figure 4: Relationship between process conditions, morphology and cellulase production.	5
Figure 5: Left: Fermentation after 8 days; Right: Fermentation after 14 days.	14
Figure 6: Calcoflour stain of straw and fungi.....	15
Figure 7: Biomass concentration after 8 days for Cre-L-AG-E1 and Cre-L-SP-E1	16
Figure 8: CLSM picture of lactose fermentations. Samples were taken after 2 and 8 days of fermentation. Top left: Cre-L-AG-E1 after 2 days; Top right: Cre-L-SP-E1 after 2 days; bottom left : Cre-L-AG-E1 after 8 days Bottom right: Cre-L-SP-E1 after 8 days	17
Figure 9: Fermentation with lactose as C-source after 24 h inoculated with pre-culture; Left: Inoculation with agar piece; Right: Inoculation with spore	18
Figure 10: Comparison of average septa length of QM-L-AG-E2, QM-L-SP-E2, Cre-L-AG-E2 and Cre-L-SP-E2	19
Figure 11: Comparison of average septa length of QM-SL-AG-E2, QM-S-SP-E2, Cre-S-AG-E2 and Cre-S-SP-E2	19
Figure 12: Left picture: QM-L-AG-E2; Right picture: QM-S-AG-E2.....	20
Figure 13: Fermentation with reduced shaking speed. Left picture: QM-L-AG-E3; Right picture: QM-S-AG-E3	21
Figure 14: Fermentation with reduced shaking speed. Left picture: QM-L-SP-E3; Right picture: QM-S-SP-E3	21
Figure 15: Comparison of QM-L-AG-E3, QM-L-SP-E3, Cre-L-AG-E3 and Cre-L-SP-E3.....	22
Figure 16: Comparison of QM-S-AG-E3, QM-S-SP-E3, Cre-S-AG-E3 and Cre-S-SP-E3	22
Figure 17: Length vs thickness at 190 rpm straw	23
Figure 18: Length vs thickness at 150 rpm straw	23
Figure 19: Length vs FPA at 190 rpm; Straw as C-source; QM9414 and Δ Cre	25
Figure 20: Length vs FPA at 150 rpm; Straw as C-source; QM9414 and Δ Cre	26
Figure 21: Thickness vs FPA 190 rpm; Straw as C-source; QM9414 and Δ Cre.....	26
Figure 22: Thickness vs FPA 150 rpm; Straw as C-source; QM9414 and Δ Cre.....	27
Figure 23: Protein concentration, Beta-Glucosidase and Xylanase activity of QM of E2.....	27
Figure 24: Protein concentration, Beta-Glucosidase and Xylanase activity of Δ Cre of E2.....	28
Figure 25: Length vs Thickness, 2L bioreactor, Spore inoculation	29
Figure 26: Determination of Protein concentration, Beta-Glucosidase activity and Xylanase activity at 2 L Bioreactor of QM	29
Figure 27: Relationship between process conditions, morphology and cellulase production	31
Figure 28: Protein concentration, Beta-Glucosidase and Xylanase activity of QM of E3.....	38
Figure 29: Protein concentration, Beta-Glucosidase and Xylanase activity of Δ Cre of E3.....	38
Figure 30: Length and thickness determination of septa with self developed software.....	39
Figure 31: 3D view of the CLSM evaluation.....	39

Figure 32: Topview of the CLSM evaluation program	40
---	----

Table

Table 1: Mineral Media (M-Media)	7
Table 2: Trace elements	7
Table 3: Carbonate-bicarbonate buffer pH 9.2 (C-buffer)	7
Table 4: Calcoflour white stain	7
Table 5: Acridin Orange	8
Table 6: β -glucosidase Assay	8
Table 7: Bradford assay	8
Table 8: Xylanase assay	8
Table 9: Dinitrosalicylic acid solution (DNS)	8
Table 10: Citrate buffer	9
Table 11: Description of Experiments conducted in this study	13
Table 12: Abbreviations.....	37

6 Index of abbreviations

Table 12: Abbreviations

TF	Transcription factor
CLSM	Confocal Laser Scanning Microscope
<i>T.reesei</i>	<i>Trichoderma reesei</i>
CBH	Cellobiohydrolase
EG	Endoglucanase
PDA	Potato dextrose Agar
p-NP	p-Nitrophenol
p-NPG	p-Nitrophenol-glucoopyranosid
KPh	Kalium Phosphate
CaCl ₂	Calcium Chloride
EtOH	Ethanol
DNS	Dinitrosalicylic acid solution
SP	Spitzenkörper
HGU	Hyphal Growth Unit

7 Appendix

7.1 Protein, beta-Glucosidase activity and xylanase activity at 150 rpm

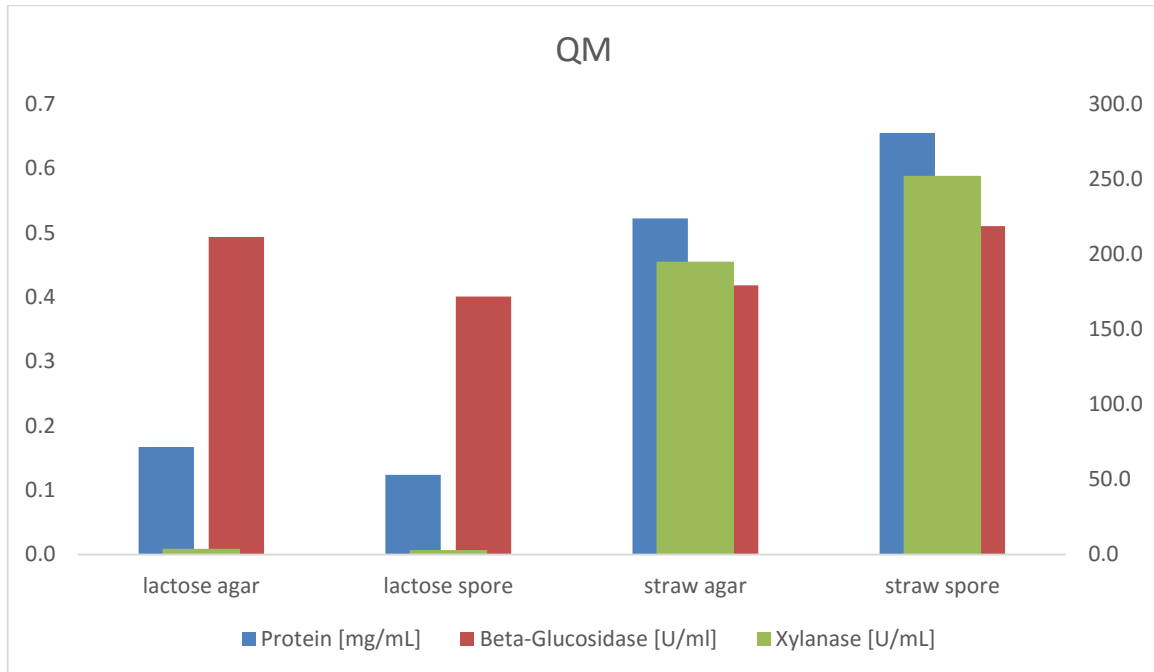


Figure 28: Protein concentration, beta-Glucosidase and xylanase activity of QM of E3

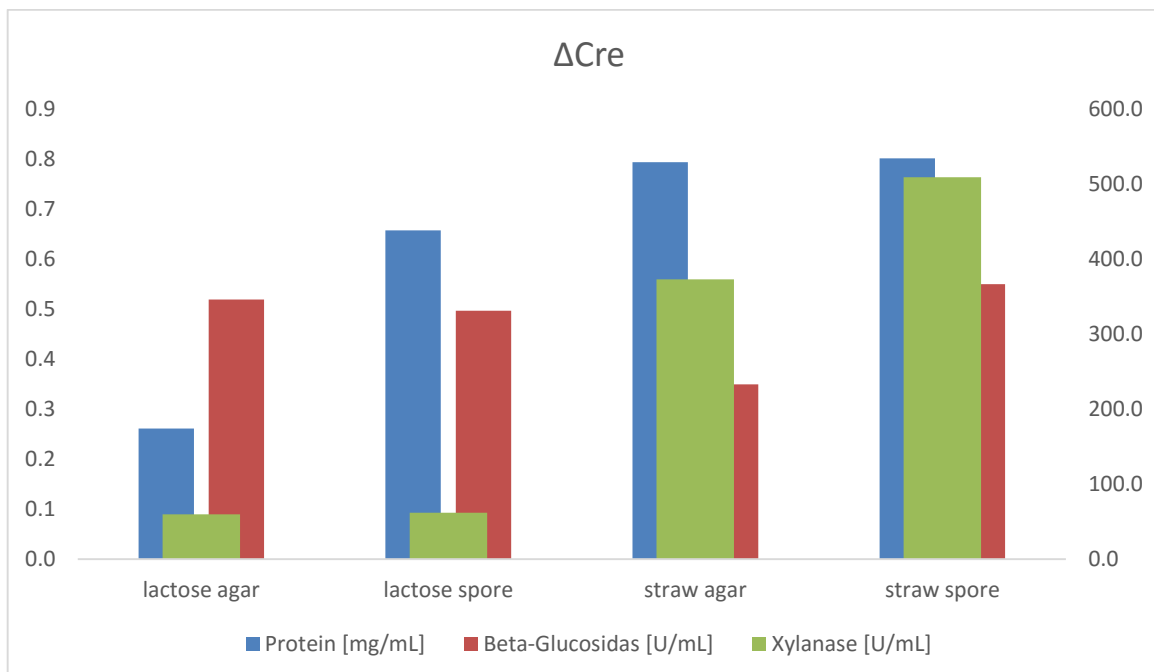


Figure 29: Protein concentration, beta-Glucosidase and xylanase activity of Δ Cre of E3

7.2 Evaluation of the CLSM picture

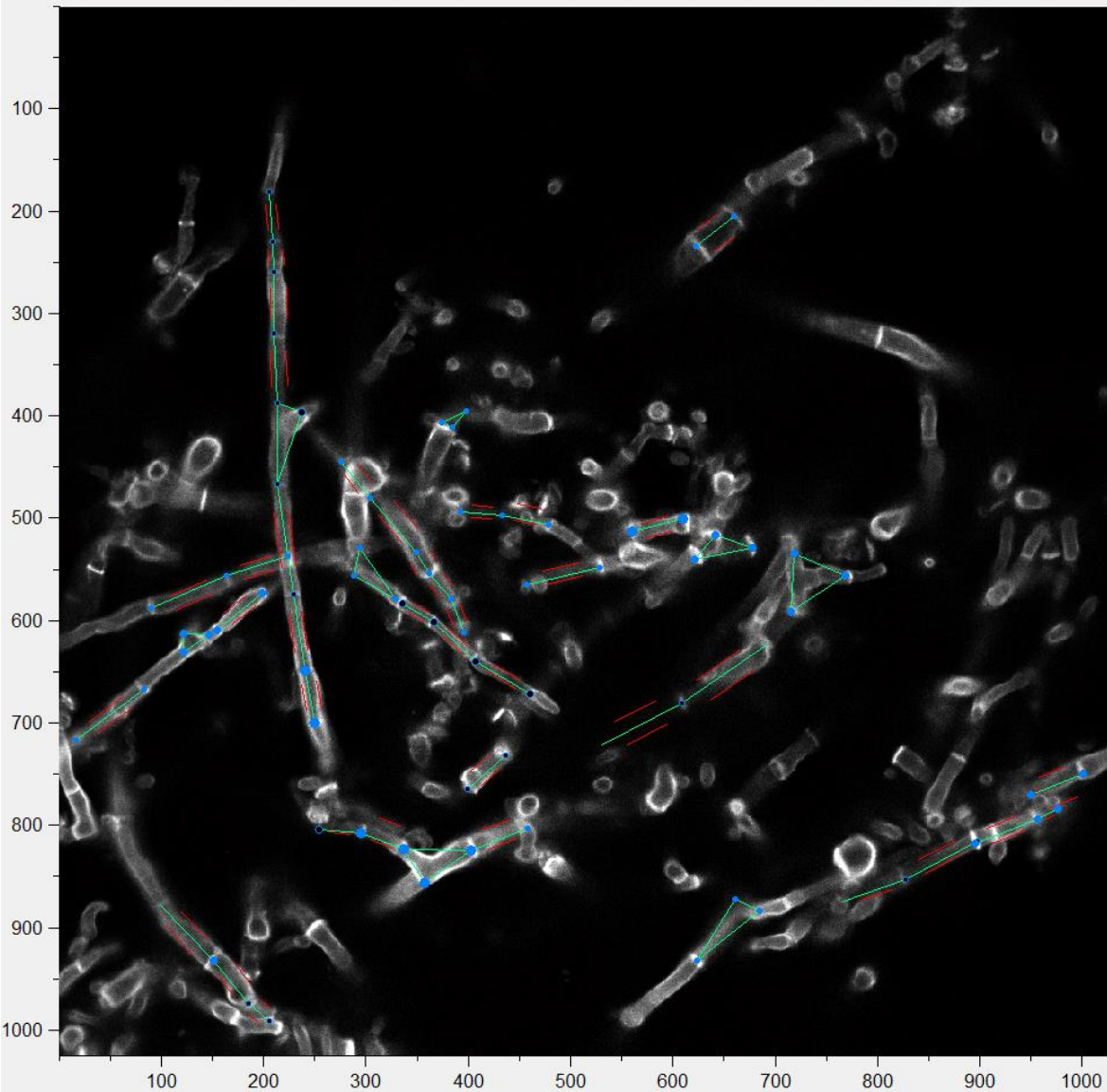


Figure 30: Length and thickness determination of septa with self developed software

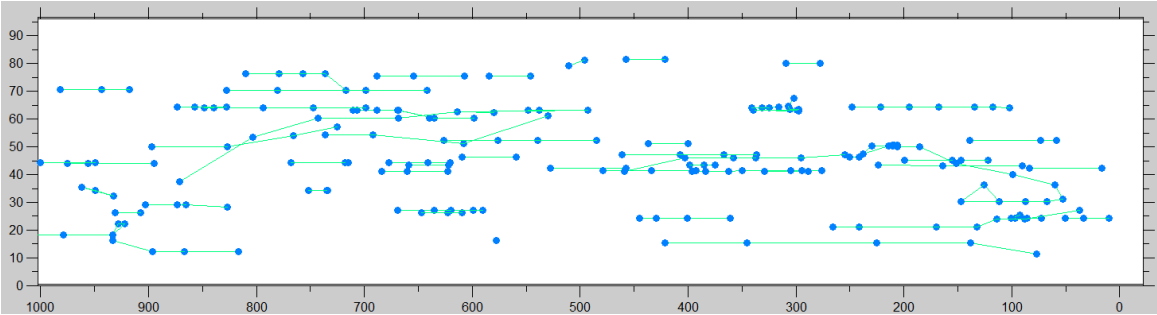


Figure 31: 3D view of the CLSM evaluation

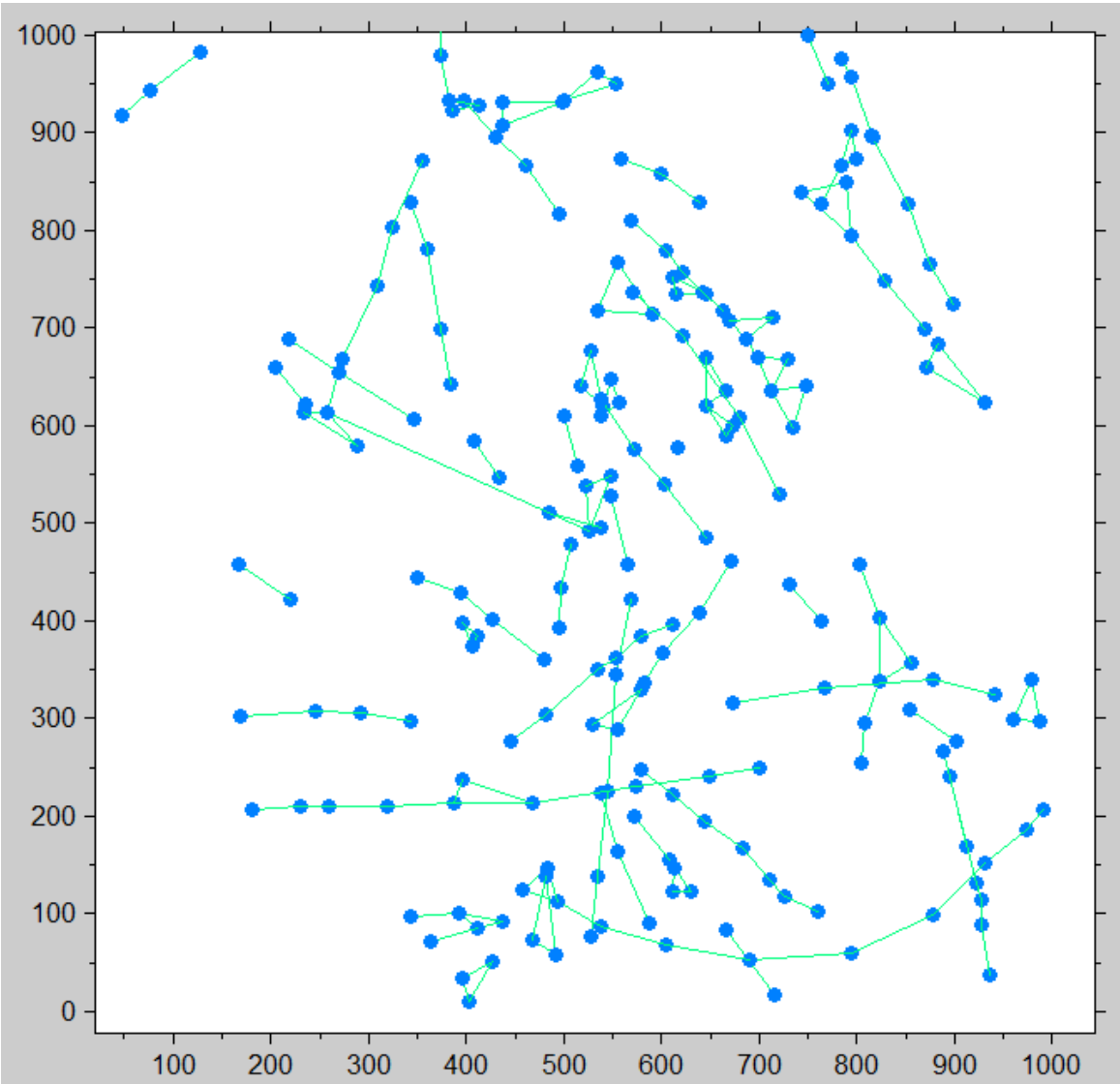


Figure 32: Topview of the CLSM evaluation program